Ramalho, G.; Tsushima, Kazuo
Octet baryon electromagnetic form factors in a relativistic quark model Physical Review D, 2011; 84(5):054014

http://link.aps.org/doi/10.1103/PhysRevD.84.054014

PHYSICAL REVIEW D **84,** 054014 (2011)

Octet baryon electromagnetic form factors in a relativistic quark model

G. Ramalho[1] and K. Tsushima[2]

[1]*CFTP, Instituto Superior Técnico, Universidade Técnica de Lisboa, Av. Rovisco Pais, 1049-001 Lisboa, Portugal*
[2]*CSSM, School of Chemistry and Physics, University of Adelaide, Adelaide SA 5005, Australia*

(Received 9 July 2011; published 16 September 2011)

We study the octet baryon electromagnetic properties by applying the covariant spectator quark model, and provide covariant parametrization that can be used to study baryon electromagnetic reactions. While we use the lattice QCD data in the large pion mass regime (small pion cloud effects) to determine the parameters of the model in the valence quark sector, we use the nucleon physical and octet baryon magnetic moment data to parametrize the pion cloud contributions. The valence quark contributions for the octet baryon electromagnetic form factors are estimated by extrapolating the lattice parametrization in the large pion mass regime to the physical regime. As for the pion cloud contributions, we parametrize them in a covariant, phenomenological manner, combined with SU(3) symmetry. We also discuss the impact of the pion cloud effects on the octet baryon electromagnetic form factors and their radii.

DOI: 10.1103/PhysRevD.84.054014 PACS numbers: 12.39.Ki, 13.40.Gp, 14.20.Dh, 14.20.Jn

I. INTRODUCTION

Low-lying baryons are classified into the octet (spin $1/2$) and decuplet (spin $3/2$) baryon members. This is based on SU(3) symmetry, which is presently understood in terms of quantum chromodynamincs (QCD). To study the electromagnetic structure of the light baryons, they are probed by electron beams, and the form factors are measured as functions of momentum transfer squared $q^2 = -Q^2$, and they reveal the nonpointlike structure of the baryons. In the octet and decuplet baryons, only the weak and electromagnetic structure of the nucleon has been well measured in experiments at finite Q^2. Our present knowledge of the electromagnetic structure for the octet and decuplet baryons is restricted to magnetic moments of some octet [1,2] and decuplet [3] baryons. Thus, except for the nucleon system [1], studies of the weak and electromagnetic structure for the other octet baryon members are very scarce [4–16]. Therefore, more data and studies of the octet baryon structure are desired.

In this work we study the electromagnetic structure of the octet baryons using the covariant spectator quark model [1–3]. In particular, one of our goals is to obtain covariant parametrization associated with the valence quark degrees of freedom, that provides insight into the octet baryon electromagnetic internal structure. This will open tremendous possibilities for future applications. A study of the decuplet baryons with the same formalism was already performed successfully in Ref. [3].

Generally, phenomenological treatment of baryon structure based solely on the valence quark degrees of freedom can be improved by the inclusion of the meson cloud effects, guided by chiral effective field theory [17]. The effects of the meson cloud are particularly important for the neutron electric form factor [1], and the electromagnetic transition, $\gamma N \to \Delta(1232)$ [18–20]. Although chiral perturbation theory is very useful to infer the Q^2 dependence of the nucleon form factors, it is usually applicable in the very low Q^2 region ($\lesssim 0.4$ GeV^2), and cannot be used to define the scale of separation between the valence quark dominant region from that of the meson-baryon excitations (meson cloud effects) [21]. The separation is possible only within a specific model. QCD in the limit of high Q^2, and many phenomenological calculations suggests that the meson cloud effects should fall off with increasing Q^2, leading to the valence quark dominance in the high Q^2 region. However, the magnitude, sign, and the rate of the falloff of the meson cloud excitations depend on models [6,21–32]. Among the mesons, the pion is expected to give the most important contributions according to chiral perturbation theory [21–23]. For example, the importance of the effects in nucleon magnetic moments in different models can be found in Ref. [2]. However, for the nucleon, an accurate description of the form factors can also be achieved by a model without the pion cloud in the physical and the lattice QCD regimes [1,33], e.g., model II in Ref. [1]. This suggests that the effects of the pion cloud can possibly be small for the nucleon form factors in the low Q^2 region. Although the pion cloud effects cannot be extracted directly from the experimental data, we assume that the octet baryon systems can be described by a mixture of the valence quarks and the pion cloud, and use lattice QCD data to constrain the valence quark contributions, and then to extract the pion cloud effects.

In this study we use the covariant spectator quark model which is inspired by the covariant spectator theory [34]. The covariant spectator quark model has been successfully applied for studying the electromagnetic properties of several baryons [1–3,18–20,33,35–44]. A baryon in the model is described by a wave function for the quark-diquark system parametrized in a covariant manner. The photon-quark coupling is described based on vector meson dominance (VMD) for a constituent quark. Because of this feature, the model can be extended easily to the lattice

QCD regime [3,20,33], as will be explained later. Starting by a simplified model for the nucleon based on an S-state configuration for the quark-diquark system, we extend the model for the octet baryons first, and next to the lattice QCD regime. That procedure allows us to use the lattice QCD simulation data with large pion masses to constrain better the parameters of the model, instead of using only the physical data. The final parametrization for the wave functions obtained in the lattice regime can then be extrapolated to obtain the physical octet baryon wave functions. This is particularly useful, since there are no experimental data for Σ, Λ, and Ξ baryons for $Q^2 > 0$. However, this procedure can only provide the contributions from the valence quarks, since still lattice QCD simulations are presently performed with large pion masses, and thus the effects of the pion cloud are suppressed [45]. To take into account the effects of the pion cloud which are very important for the physical regime, we first use a simple, covariant parametrization for the pion cloud contributions for the nucleon electromagnetic form factors. Then, the parametrization for the nucleon is extended to the other octet baryon members using SU(3) symmetry.

This article is organized as follows. In Sec. II we describe the electromagnetic current, and discuss the separation of the photon couplings with the quarks, and those with the pion cloud. In Sec. III we give detailed explanations of the covariant spectator quark model extended for the octet baryons, both for the physical and lattice QCD regimes. In Sec. IV we discuss the pion cloud contributions, and give phenomenological parametrization for the pion cloud contributions. In Sec. V explicit parametrization for the octet baryon wave functions and pion cloud contributions for the electromagnetic form factors are presented. The results for the bare and dressed electromagnetic form factors of the octet baryons are presented in Sec. VI. Summary and conclusions are given in Sec. VII.

II. VALENCE QUARK AND PION CLOUD CONTRIBUTIONS FOR THE CURRENT

The current associated with the elastic electromagnetic interaction with a baryon B, with spin $1/2$ positive parity and mass M_B, can be represented in general as

$$J_B^\mu = F_{1B}(Q^2)\gamma^\mu + F_{2B}(Q^2)\frac{i\sigma^{\mu\nu}q_\nu}{2M_B}, \tag{1}$$

where F_{1B} and F_{2B} are, respectively, the Dirac and Pauli form factors which are the functions of $Q^2 = -q^2$, where $q = P_+ - P_-$, with P_+ (P_-) being the final (initial) momentum. Omitted in Eq. (1) are the initial and final state Dirac spinors function of $P_\pm$ and the spin projections. For simplicity we represent the current in units $e = \sqrt{4\pi\alpha}$, with $\alpha \simeq 1/137$, the electromagnetic fine structure constant. At $Q^2 = 0$, these form factors are defined as

$$F_{1B}(0) = e_B, \qquad F_{2B}(0) = \kappa_B, \tag{2}$$

where e_B is the baryon charge in units of e and κ_B is the baryon anomalous magnetic moment in natural units $\frac{e}{2M_B}$. An alternative representation of the electromagnetic form factors of the baryon B is the Sachs parametrization in terms of the electric charge $G_{EB} = F_{1B} - \frac{Q^2}{4M_B^2}F_{2B}$ and magnetic dipole $G_{MB} = F_{1B} + F_{2B}$ form factors.

In a quark model the electromagnetic interaction with a baryon B may be decomposed into the photon interaction with valence quarks, and with sea quarks (polarized quark-antiquark pairs). The latter can be interpreted as virtual mesons which dress the baryon valence quark core. The photon couplings with the intermediate meson-baryon states can be described by effective field theories that are perturbative for the low meson energies and momenta. According to chiral perturbation theory, the most important meson for a given reaction is the lightest one, the pion. This is also expected to be the case for the octet baryons. Thus, we can describe the electromagnetic interaction for a member B of the octet baryons using a current,

$$J_B^\mu = Z_B[J_{0B}^\mu + J_\pi^\mu + J_{\gamma B}^\mu], \tag{3}$$

where J_{0B}^μ stands for the electromagnetic interaction with the quark core without the pion cloud, and the remaining terms are the interaction with the intermediate pion-baryon (πB) states. (See Fig. 1.) In particular, J_π^μ represents the direct interaction with the pion, and $J_{\gamma B}^\mu$ the interaction with the baryon while one pion is in the air. The factor Z_B is a renormalization constant, which is common to each isomultiplet: nucleon (N), Σ, Λ, and Ξ. Z_B is related with the derivative of the baryon self-energy [2].

In an additive constituent quark model, the current J_{0B}^μ is given by the sum of the individual quark current. The electromagnetic interaction processes for the nucleon in the covariant spectator quark model [1] is presented in Fig. 2. The decomposition Eq. (3) is justified when the pion is created by the *overall baryon*, but not by a single

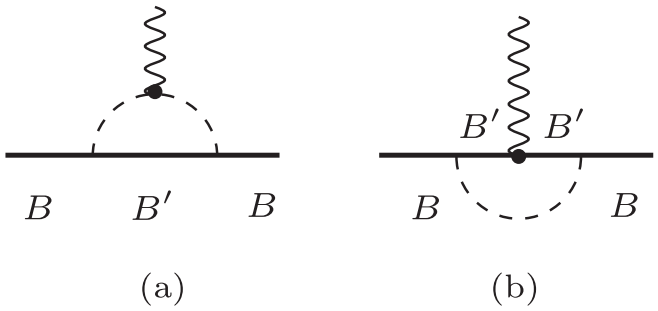

FIG. 1. Electromagnetic interaction with the baryon B within the one-pion loop level (pion cloud) through the intermediate baryon states B'. A diagram including a contact vertex $\gamma\pi BB'$, as described in Ref. [2], is not represented explicitly, since the isospin structure is the same as diagram (a). See Ref. [2] for details.

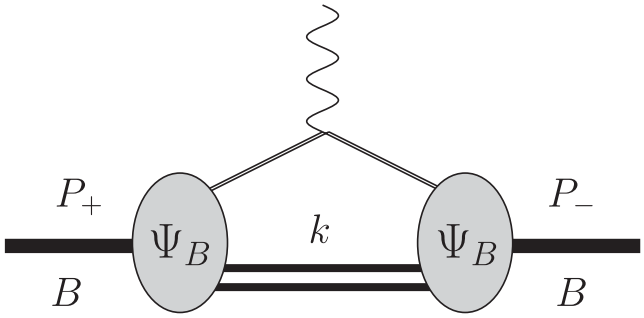

FIG. 2. Electromagnetic interaction with the baryon B in an impulse approximation. P_+ (P_-) represents the final (initial) baryon momentum and k the momentum of the on-shell diquark. The baryon wave function is represented by Ψ_B.

quark. The processes where pions are created and absorbed by the same quark are included in the constituent quark internal structure, and thus included in the current J^μ_{0B}.

III. SPECTATOR QUARK MODEL FOR THE OCTET BARYONS

In the covariant spectator quark model a baryon B is described as a system with an off-mass-shell quark, free to interact with photons, and two on-mass-shell quarks. Integrating over the two on-mass-shell quark momenta, we represent the quark pair as an on-mass-shell diquark with an effective mass m_D, and the baryon as a quark-diquark system [1]. This quark-diquark system is then described by a transition vertex between the three-quark bound state and the quark-diquark state, that describes effectively the confinement [1,3].

A. Octet baryon wave functions

The simplest representation for a quark-diquark system with spin $1/2$ and positive parity is the S-wave configuration. The wave function for an octet baryon B with momentum P and the internal diquark momentum k, can be represented in the S-state approximation [1,2],

$$\Psi_B(P,k) = \frac{1}{\sqrt{2}}\{\phi_S^0|M_A\rangle + \phi_S^1|M_S\rangle\}\psi_B(P,k), \quad (4)$$

where $|M_A\rangle$ and $|M_S\rangle$ are the flavor antisymmetric and mixed symmetric states, respectively, and $\phi_S^{0,1}$ are the spin (0 and 1) wave functions. $\psi_B(P,k)$ is a scalar function of P and k, and it reflects the momentum distribution of the quark-diquark system.

Explicit baryon flavor wave functions are presented in Table I. The spin wave functions are given by [1]

$$\phi_S^0\left(+\frac{1}{2}\right) = \frac{1}{\sqrt{2}}(\uparrow\downarrow - \downarrow\uparrow)\uparrow, \quad (5)$$

$$\phi_S^1\left(+\frac{1}{2}\right) = -\frac{1}{\sqrt{6}}[(\uparrow\downarrow + \downarrow\uparrow)\uparrow - 2\uparrow\uparrow\downarrow], \quad (6)$$

and

$$\phi_S^0\left(-\frac{1}{2}\right) = \frac{1}{\sqrt{2}}(\uparrow\downarrow - \downarrow\uparrow)\downarrow, \quad (7)$$

$$\phi_S^1\left(-\frac{1}{2}\right) = \frac{1}{\sqrt{6}}[(\uparrow\downarrow + \downarrow\uparrow)\downarrow - 2\downarrow\downarrow\uparrow]. \quad (8)$$

This nonrelativistic structure is generalized in the covariant spectator quark model [1] as

$$\phi_S^0 = u_B(P,s), \qquad \phi_S^1 = -\varepsilon_\lambda^{\alpha *}(P)U_B^\alpha(P,s), \quad (9)$$

where

$$U_B^\alpha(P,s) = \frac{1}{\sqrt{3}}\gamma_5\left(\gamma^\alpha - \frac{P^\alpha}{M}\right)u_B(P,s). \quad (10)$$

In the above $u_B(P,s)$ is the Dirac spinor of the octet baryon B with momentum P, spin s, and $\varepsilon_\lambda(P)$ the diquark polarization in the fixed-axis representation [1,35]. In Ref. [1] it is shown how Eq. (9) generalizes the nonrelativistic spin wave functions.

B. Electromagnetic current

Taking into account that the wave function Ψ_B is written in terms of the wave functions of a quark pair (12) and a

TABLE I. Flavor wave functions of the octet baryons.

B	$\lvert M_S\rangle$	$\lvert M_A\rangle$
p	$\frac{1}{\sqrt{6}}[(ud+du)u - 2uud]$	$\frac{1}{\sqrt{2}}(ud-du)u$
n	$-\frac{1}{\sqrt{6}}[(ud+du)d - 2ddu]$	$\frac{1}{\sqrt{2}}(ud-du)d$
Λ^0	$\frac{1}{2}[(dsu-usd)+s(du-ud)]$	$\frac{1}{\sqrt{12}}[s(du-ud)-(dsu-usd)-2(du-du)s]$
Σ^+	$\frac{1}{\sqrt{6}}[(us+su)u - 2uus]$	$\frac{1}{\sqrt{2}}(us-su)u$
Σ^0	$\frac{1}{\sqrt{12}}[s(du+ud)+(dsu+usd)-2(ud+du)s]$	$\frac{1}{2}[(dsu+usd)-s(ud+du)]$
Σ^-	$\frac{1}{\sqrt{6}}[(sd+ds)d - 2dds]$	$\frac{1}{\sqrt{2}}(ds-sd)d$
Ξ^0	$-\frac{1}{\sqrt{6}}[(ud+du)s - 2ssu]$	$\frac{1}{\sqrt{2}}(us-su)s$
Ξ^-	$-\frac{1}{\sqrt{6}}[(ds+sd)s - 2ssd]$	$\frac{1}{\sqrt{2}}(ds-sd)s$

single quark (3), one can write the electromagnetic current associated with the baryon B in a impulse approximation [1,3],

$$J^{\mu}_{0B} = 3\sum_{\Gamma}\int_{k}\bar{\Psi}_{B}(P_{+},k)j^{\mu}_{q}\Psi_{B}(P_{-},k), \tag{11}$$

where j^{μ}_{q} is the quark current operator, P_{+} (P_{-}) is the final (initial) baryon momentum and k the momentum of the on-shell diquark, and $\Gamma = \{s, \lambda\}$ labels the scalar diquark and the vectorial diquark polarization $\lambda = 0, \pm$. The factor 3 in Eq. (11) takes into account the contributions for the current from the pairs (13) and (23), where each pair has the identical contribution with that of the pair (12). The polarization indices are suppressed for simplicity. The integral symbol represents

$$\int_{k} = \int\frac{d^{3}\mathbf{k}}{2E_{D}(2\pi)^{3}}, \tag{12}$$

where $E_{D} = \sqrt{m_{D}^{2} + \mathbf{k}^{2}}$.

Generally, the baryon electromagnetic current (11) can be expressed as

$$J^{\mu}_{0B} = \tilde{e}_{0B}\gamma^{\mu} + \tilde{\kappa}_{0B}\frac{i\sigma^{\mu\nu}q_{\nu}}{2M_{B}}, \tag{13}$$

where $\tilde{e}_{0B}$ and $\tilde{\kappa}_{0B}$ are the functions of Q^{2}, and, respectively, correspond to the valence quark contributions for the $F_{1B}(Q^{2})$ and $F_{2B}(Q^{2})$ form factors. To represent these quantities for $Q^{2} = 0$, we suppress the tildes. Note that in Eq. (13) we omit the baryon spinors as in Eq. (1).

C. Quark current

The quark current operator j^{μ}_{q} has a generic structure,

$$j^{\mu}_{q} = j_{1}\left(\gamma^{\mu} - \frac{\not{q}q^{\mu}}{q^{2}}\right) + j_{2}\frac{i\sigma^{\mu\nu}q_{\nu}}{2M_{N}}, \tag{14}$$

where M_{N} is the nucleon mass and j_{i} ($i = 1, 2$) are SU(3) flavor operators acting on the third quark of the $|M_{A}\rangle$ or $|M_{S}\rangle$ state. In the first term $\not{q}q^{\mu}/q^{2}$ is included for completeness, but does not contribute for elastic reactions.

The quark current j_{i} ($i = 1, 2$) in Eq. (14), can be decomposed as the sum of operators acting on quark 3 in SU(3) flavor space,

$$j_{i} = \frac{1}{6}f_{i+}\lambda_{0} + \frac{1}{2}f_{i-}\lambda_{3} + \frac{1}{6}f_{i0}\lambda_{s}, \tag{15}$$

where

$$\lambda_{0} = \begin{pmatrix}1&0&0\\0&1&0\\0&0&0\end{pmatrix}, \quad \lambda_{3} = \begin{pmatrix}1&0&0\\0&-1&0\\0&0&0\end{pmatrix}, \quad \lambda_{s} \equiv \begin{pmatrix}0&0&0\\0&0&0\\0&0&-2\end{pmatrix} \tag{16}$$

TABLE II. Mixed symmetric and antisymmetric coefficients for the octet baryons appearing in Eqs. (17) and (18).

B	j^{S}_{i}	j^{A}_{i}
p	$\frac{1}{6}(f_{i+} - f_{i-})$	$\frac{1}{6}(f_{i+} + 3f_{i-})$
n	$\frac{1}{6}(f_{i+} + f_{i-})$	$\frac{1}{6}(f_{i+} - 3f_{i-})$
Λ^{0}	$\frac{1}{6}f_{i+}$	$\frac{1}{18}(f_{i+} - 4f_{i0})$
Σ^{+}	$\frac{1}{18}(f_{i+} + 3f_{i-} - 4f_{i0})$	$\frac{1}{6}(f_{i+} + 3f_{i-})$
Σ^{0}	$\frac{1}{36}(2f_{i+} - 8f_{i0})$	$\frac{1}{6}f_{i+}$
Σ^{-}	$\frac{1}{18}(f_{i+} - 3f_{i-} - 4f_{i0})$	$\frac{1}{6}(f_{i+} - 3f_{i-})$
Ξ^{0}	$\frac{1}{18}(2f_{i+} + 6f_{i-} - 2f_{i0})$	$-\frac{1}{3}f_{i0}$
Ξ^{-}	$\frac{1}{18}(2f_{i+} - 6f_{i-} - 2f_{i0})$	$-\frac{1}{3}f_{i0}$

are the flavor operators. These operators act on the quark wave function in flavor space, $q = (uds)^{T}$.

The functions $f_{i\pm}(Q^{2})$ ($i = 1, 2$) are normalized by $f_{1n}(0) = 1$ ($n = 0, \pm$), $f_{2\pm}(0) = \kappa_{\pm}$, and $f_{20}(0) = \kappa_{s}$. The isoscalar (κ_{+}) and isovector (κ_{-}) anomalous magnetic moments are defined in terms of the u and d quark anomalous magnetic moments, $\kappa_{+} = 2\kappa_{u} - \kappa_{d}$ and $\kappa_{-} = \frac{2}{3}\kappa_{u} + \frac{1}{3}\kappa_{d}$. In the previous works the quark anomalous magnetic moments were adjusted to reproduce the experimental magnetic moments of the nucleon and the Ω^{-} [1,3]. In this work however, we will readjust the u and d quark anomalous magnetic moments as will be explained later.

To see explicitly the quark flavor contributions for the electromagnetic current (14), we sum over the quark flavors following Refs. [2,3], and get the coefficients

$$j^{A}_{i} = \langle M_{A}|j_{i}|M_{A}\rangle, \tag{17}$$

$$j^{S}_{i} = \langle M_{S}|j_{i}|M_{S}\rangle, \tag{18}$$

for $i = 1, 2$. The results, corresponding to the states given in Table I, are presented in Table II.

D. Valence quark contributions for the electromagnetic form factors

Using the expressions derived in the previous work for the nucleon form factors in the S-state approach [1], we obtain the corresponding expressions for the octet baryons B by replacing the nucleon coefficients j^{A}_{i} and j^{S}_{i} ($i = 1, 2$) by the respective baryon state,

$$\tilde{e}_{0B} = B(Q^{2}) \times \left(\frac{3}{2}j^{A}_{1} + \frac{1}{2}\frac{3-\tau}{1+\tau}j^{S}_{1} - 2\frac{\tau}{1+\tau}\frac{M_{B}}{M_{N}}j^{S}_{2}\right), \tag{19}$$

$$\tilde{\kappa}_{0B} = B(Q^{2}) \times \left[\left(\frac{3}{2}j^{A}_{2} - \frac{1}{2}\frac{1-3\tau}{1+\tau}j^{S}_{2}\right)\frac{M_{B}}{M_{N}} - 2\frac{1}{1+\tau}j^{S}_{1}\right], \tag{20}$$

with $\tau = \frac{Q^2}{4M_B^2}$, and

$$B(Q^2) = \int_k \psi_B(P_+, k)\psi_B(P_-, k) \tag{21}$$

the overlap integral between the initial and final scalar wave functions. The normalization of the wave function leads to $B(0) = 1$. The expressions in Eqs. (19) and (20) given for the nucleon [1] are briefly reviewed in the Appendix.

Another possible electromagnetic transition between the octet baryon members is $\gamma^*\Lambda \to \Sigma^0$. This transition is very interesting, and will be studied in a separate work [46], since it is an inelastic reaction.

The expressions for $\tilde{e}_{0B}$ and $\tilde{\kappa}_{0B}$ [Eqs. (19) and (20)] are particularly simplified for $Q^2 = 0$,

$$e_{0B} = \frac{3}{2}(j_1^A + j_1^S), \quad \kappa_{0B} = \left(\frac{3}{2}j_2^A - \frac{1}{2}j_2^S\right)\frac{M_N}{M_B} - 2j_1^S. \tag{22}$$

We require that the bare charge e_{0B} and the dressed charge e_B are the same,

$$e_{0B} = e_B. \tag{23}$$

To get the numerical results, we must specify the functions $f_{\text{in}}(Q^2)$ ($i = 1, 2$, $n = 0, \pm$) and $\psi_B(P, k)$. The explicit expressions will be given in Sec. V.

The form factors described in this section, corresponding to Eqs. (19) and (20), include only the valence quark contributions. For a realistic estimate we need to include the pion cloud effects explicitly.

IV. PION CLOUD CONTRIBUTIONS FOR THE ELECTROMAGNETIC FORM FACTORS

We discuss here the pion cloud contributions for the electromagnetic current and form factors, represented by the diagrams in Fig. 1. Following Ref. [2], we assume the pion as the dominant meson excitation to be included in the octet baryon form factors. Then, the meson cloud contributions for the octet baryon electromagnetic form factors can be described in terms of 6 independent functions of Q^2, related to the pion-baryon Feynman integral, as will be described next.

A. Pion-baryon couplings in SU(3)

The meson-baryon interaction vertices between the baryon octet and the pseudoscalar meson octet, π, K, $\bar{K}$, and η, can be described by the two independent coefficients D and F based on SU(3) symmetry [47,48]. The coupling constant of the pion (π) and baryons (B and B'), $g_{\pi BB'}$, can be represented in terms of the ratio $\alpha = \frac{D}{F+D}$ and a global coupling constant $g = g_{\pi NN}$, the πNN coupling constant. As a result, the interaction currents and baryon self-energies, at the one-pion loop level, which depend on the coupling constants of πNN, $\pi\Lambda\Sigma$, $\pi\Sigma\Sigma$ and $\pi\Xi\Xi$, can be expressed in terms of the independent coefficients β_B for $B = \Lambda, \Sigma, \Xi$,

$$\beta_\Lambda = \frac{4}{3}\alpha^2, \tag{24}$$

$$\beta_\Sigma = 4(1-\alpha)^2, \tag{25}$$

$$\beta_\Xi = (1-2\alpha)^2. \tag{26}$$

The factor for the nucleon is $\beta_N = 1$. Absorbing the global coupling constant g in the functions associated with the pion-baryon loops, we can express the pion cloud contributions entirely in terms of α.

In the exact SU(3) symmetry limit all the octet baryon masses are the same. We break the symmetry by the pion cloud effects on the mass, but only by the one-pion loop in the self-energies. Following Ref. [2], we represent the mass of the octet baryon B as $M_B = M_0 + \Sigma(M_B)$, where M_0 is a mass parameter and $\Sigma(M_B)$ the self-energy at the physical baryon mass point. Then, we can write $\Sigma(M_B) = G_{0B}\mathcal{B}_0$, with $\mathcal{B}_0$ being a scalar integral and G_{0B} a factor that includes the couplings of the pion with the baryon (see Table 2 in Ref. [2]). Using the value, $\alpha = 0.6$ given by an SU(6) quark model [24], we get $M_0 = 1.342$ GeV and $\mathcal{B}_0 = -0.127$ GeV, which can describe the octet baryon masses within an accuracy of 7%.

The choice of $\alpha = 0.6$ given by SU(6) symmetry, defines the strength of the pion cloud contributions as $\beta_\Sigma = \frac{16}{25}$, $\beta_\Lambda = \frac{12}{25}$, and $\beta_\Xi = \frac{1}{25}$ [6,24]. Note that, the intermediate baryons in the one-pion loop diagrams in Fig. 1 are always those in the same isomultiplet with the external baryons (N, Σ, or Ξ), with the exception of the Λ-Σ mixture for the Σ case, where the mass difference of them is small.

A comment on the value of α is in order. Contrary to the previous study of the spectator quark model [2], where $\alpha \simeq 0.69$ was obtained by fitting to the octet baryon masses and octet baryon magnetic moments, here we use the value obtained by SU(6) symmetry. This enables us to treat all the octet and decuplet baryons in a unified manner based on SU(6) symmetry.

B. Pion cloud dressing

The pion cloud corrections, namely, the coupling of the photon to the pion J^μ_π, and the coupling to the intermediate baryons $J^\mu_{\gamma B}$, can be written [2]

$$J^\mu_\pi = \left(\tilde{B}_1\gamma^\mu + \tilde{B}_2\frac{i\sigma^{\mu\nu}q_\nu}{2M_B}\right)G_{\pi B}, \tag{27}$$

$$J^\mu_{\gamma B} = \left(\tilde{C}_1\gamma^\mu + \tilde{C}_2\frac{i\sigma^{\mu\nu}q_\nu}{2M_B}\right)G_{eB} + \left(\tilde{D}_1\gamma^\mu + \tilde{D}_2\frac{i\sigma^{\mu\nu}q_\nu}{2M_B}\right)G_{\kappa B}. \tag{28}$$

In the above, $\tilde{B}_i$, $\tilde{C}_i$, and $\tilde{D}_i$ ($i = 1, 2$) are arbitrary functions of Q^2 (as $\tilde{e}_{0B}$ and $\tilde{\kappa}_{0B}$ are), and $G_{\pi B}$, G_{eB}, $G_{\kappa B}$ are the coefficients that depend on the baryon flavors

TABLE III. Coefficients $G_{\pi B}$ and G_{zB}, where $z = e, \kappa$ for the octet baryons $B = N, \Lambda, \Sigma$, and Ξ. See also Ref. [2] for details.

B	$G_{\pi B}$	G_{zB}
N	$2\tau_3$	$\frac{1}{2}(3z_N^s - z_N^v)$
Λ	0	$\beta_\Lambda(3z_\Sigma^0 + z_\Sigma^2)$
Σ	$(\beta_\Sigma + \beta_\Lambda)\mathbf{J}_3$	$[\beta_\Sigma(2z_\Sigma^0 + z_\Sigma^2) + \beta_\Lambda z_\Lambda]\mathbf{1} + \frac{1}{2}\beta_\Sigma(z_\Sigma^1\mathbf{J}_3 - z_\Sigma^2\mathbf{J}_3^2)$
Ξ	$2\beta_\Xi\tau_3$	$\beta_\Xi(3z_\Xi^s - z_\xi^v\tau_3)$

($B = N, \Sigma, \Lambda, \Xi$). We assume that the functions $\tilde{B}_i$, $\tilde{C}_i$, and $\tilde{D}_i$ are only weakly dependent on the baryon masses, and the same for all the octet baryons as in Ref. [2]. That allows a description of the pion cloud dressing with a reduced number of coefficients. We write B_i, C_i, and D_i to represent, respectively, the functions $\tilde{B}_i$, $\tilde{C}_i$, and $\tilde{D}_i$ at $Q^2 = 0$. The coefficients $\tilde{B}_1$ and $\tilde{B}_2$ are proportional to the pion electromagnetic form factor $F_\pi(Q^2)$, but we absorb it in the definitions of $\tilde{B}_i$ for simplicity.

Combining Eqs. (3), (27), and (28), we get

$$J_B^\mu = Z_B\{\tilde{e}_{0B} + G_{\pi B}\tilde{B}_1 + G_{eB}\tilde{C}_1 + G_{\kappa B}\tilde{D}_1\}\gamma^\mu + Z_B\{\tilde{\kappa}_{0B} + G_{\pi B}\tilde{B}_2 + G_{eB}\tilde{C}_2 + G_{\kappa B}\tilde{D}_2\}\frac{i\sigma^{\mu\nu}q_\nu}{2M_B}. \tag{29}$$

The renormalization constant Z_B is determined by the relation between the dressed form factor F_{1B} at $Q^2 = 0$ and the charge e_B [$F_{1B}(0) = e_B$], or by the self-energy. (See Ref. [2] for details.) The condition for the nucleon leads to

$$D_1 = 0, \qquad B_1 = C_1, \tag{30}$$

and gives

$$Z_N = [1 + 3B_1]^{-1}. \tag{31}$$

Similarly, we can get the renormalization constants for the other octet baryons [2]

$$\begin{aligned} Z_\Lambda &= [1 + 3\beta_\Lambda B_1]^{-1}, \\ Z_\Sigma &= [1 + (2\beta_\Sigma + \beta_\Lambda)B_1]^{-1}, \\ Z_\Xi &= [1 + 3\beta_\Xi B_1]^{-1}. \end{aligned} \tag{32}$$

C. Coefficients $G_{\pi B}$, G_{eB} and $G_{\kappa B}$

The coefficients $G_{\pi B}$ and G_{zB}, where z is either e or κ, were calculated in Ref. [2]. To express the results, it is convenient to introduce a general operator decomposition for the bare current. We use z_B to represent $\tilde{e}_B$ or $\tilde{\kappa}_B$. For the N and Ξ isospin doublets, we use the standard isoscalar-isovector notation,

$$z_B = \frac{1}{2}(z_B^s + z_B^v\tau_3). \tag{33}$$

At $Q^2 = 0$ we have $e_N^s = e_N^v = 1$, and $e_\Xi^s = -e_\Xi^v = -1$. The Λ case is given by the scalar functions $\tilde{e}_{0\Lambda}$ and $\tilde{\kappa}_{0\Lambda}$, with $e_\Lambda = e_{0\Lambda} = 0$.

For the Σ isospin operators, the decomposition of the three states (0, $\pm$) can be given by

$$z_\Sigma = z_\Sigma^0\mathbf{1} + \frac{1}{2}(z_\Sigma^1\mathbf{J}_3 + z_\Sigma^2\mathbf{J}_3^2), \tag{34}$$

where $\mathbf{J}_3$ is the third component of the isospin 1 operator. With this notation we get

$$\begin{aligned} z_\Sigma^0 &= z_{\Sigma^0}, \qquad z_\Sigma^1 = z_{\Sigma^+} - z_{\Sigma^-}, \\ z_\Sigma^2 &= z_{\Sigma^+} + z_{\Sigma^-} - 2z_{\Sigma^0}, \end{aligned} \tag{35}$$

where $e_\Sigma^0 = e_\Sigma^2 = 0$ and $e_\Sigma^1 = 2$, for $Q^2 = 0$. The results for the coefficients are listed in Table III. (See Ref. [2] for details.)

D. Octet baryon electromagnetic form factors with pion cloud dressing

From the current (29), using the expressions (19) and (20), and the coefficients in Table III, we can write down the Dirac form factors F_{1B} for the octet baryons B,

$$F_{1p} = Z_N\{\tilde{e}_{0p} + 2\tilde{B}_1 + (\tilde{e}_{0p} + 2\tilde{e}_{0n})\tilde{C}_1 + (\tilde{\kappa}_{0p} + 2\tilde{\kappa}_{0n})\tilde{D}_1\}, \tag{36}$$

$$F_{1n} = Z_N\{\tilde{e}_{0n} - 2\tilde{B}_1 + (2\tilde{e}_{0p} + \tilde{e}_{0n})\tilde{C}_1 + (2\tilde{\kappa}_{0p} + \tilde{\kappa}_{0n})\tilde{D}_1\}, \tag{37}$$

$$F_{1\Lambda} = Z_\Lambda\{\tilde{e}_{0\Lambda} + \beta_\Lambda(\tilde{e}_{0\Sigma^+} + \tilde{e}_{0\Sigma^0} + \tilde{e}_{0\Sigma^-})\tilde{C}_1 + \beta_\Lambda(\tilde{\kappa}_{0\Sigma^+} + \tilde{\kappa}_{0\Sigma^0} + \tilde{\kappa}_{0\Sigma^-})\tilde{D}_1\}, \tag{38}$$

$$F_{1\Sigma^+} = Z_\Sigma\{\tilde{e}_{0\Sigma^+} + (\beta_\Sigma + \beta_\Lambda)\tilde{B}_1 + [\beta_\Sigma(\tilde{e}_{0\Sigma^+} + \tilde{e}_{0\Sigma^0}) + \beta_\Lambda\tilde{e}_{0\Lambda}]\tilde{C}_1 + [\beta_\Sigma(\tilde{\kappa}_{0\Sigma^+} + \tilde{\kappa}_{0\Sigma^0}) + \beta_\Lambda\tilde{\kappa}_{0\Lambda}]\tilde{D}_1\}, \tag{39}$$

$$F_{1\Sigma^0} = Z_\Sigma\{\tilde{e}_{0\Sigma^0} + [\beta_\Sigma(\tilde{e}_{0\Sigma^+} + \tilde{e}_{0\Sigma^-}) + \beta_\Lambda\tilde{e}_{0\Lambda}]\tilde{C}_1 + [\beta_\Sigma(\tilde{\kappa}_{0\Sigma^+} + \tilde{\kappa}_{0\Sigma^-}) + \beta_\Lambda\tilde{\kappa}_{0\Lambda}]\tilde{D}_1\}, \tag{40}$$

$$F_{1\Sigma^-} = Z_\Sigma\{\tilde{e}_{0\Sigma^-} - (\beta_\Sigma + \beta_\Lambda)\tilde{B}_1 + [\beta_\Sigma(\tilde{e}_{0\Sigma^0} + \tilde{e}_{0\Sigma^-}) + \beta_\Lambda\tilde{e}_{0\Lambda}]\tilde{C}_1 + [\beta_\Sigma(\tilde{\kappa}_{0\Sigma^0} + \tilde{\kappa}_{0\Sigma^-}) + \beta_\Lambda\tilde{\kappa}_{0\Lambda}]\tilde{D}_1\}, \quad (41)$$

$$F_{1\Xi^0} = Z_\Sigma\{\tilde{e}_{0\Xi^0} + 2\beta_\Xi\tilde{B}_1 + \beta_\Xi(\tilde{e}_{0\Xi^0} + 2\tilde{e}_{0\Xi^-})\tilde{C}_1 + \beta_\Xi(\tilde{\kappa}_{0\Xi^0} + 2\tilde{\kappa}_{0\Xi^-})\tilde{D}_1\}, \quad (42)$$

$$F_{1\Xi^-} = Z_\Sigma\{\tilde{e}_{0\Xi^-} - 2\beta_\Xi\tilde{B}_1 + \beta_\Xi(2\tilde{e}_{0\Xi^0} + \tilde{e}_{0\Xi^-})\tilde{C}_1 + \beta_\Xi(2\tilde{\kappa}_{0\Xi^0} + \tilde{\kappa}_{0\Xi^-})\tilde{D}_1\}. \quad (43)$$

Similarly, for the Pauli form factors F_{2B}, we can write down

$$F_{2p} = Z_N\{\tilde{\kappa}_{0p} + 2\tilde{B}_2 + (\tilde{e}_{0p} + 2\tilde{e}_{0n})\tilde{C}_2 + (\tilde{\kappa}_{0p} + 2\tilde{\kappa}_{0n})\tilde{D}_2\}, \quad (44)$$

$$F_{2n} = Z_N\{\tilde{\kappa}_{0n} - 2\tilde{B}_2 + (2\tilde{e}_{0p} + \tilde{e}_{0n})\tilde{C}_2 + (2\tilde{\kappa}_{0p} + \tilde{\kappa}_{0n})\tilde{D}_2\}, \quad (45)$$

$$F_{2\Lambda} = Z_\Lambda\{\tilde{\kappa}_{0\Lambda} + \beta_\Lambda(\tilde{e}_{0\Sigma^+} + \tilde{e}_{0\Sigma^0} + \tilde{e}_{0\Sigma^-})\tilde{C}_2 + \beta_\Lambda(\tilde{\kappa}_{0\Sigma^+} + \tilde{\kappa}_{0\Sigma^0} + \tilde{\kappa}_{0\Sigma^-})\tilde{D}_2\}, \quad (46)$$

$$F_{2\Sigma^+} = Z_\Sigma\{\tilde{\kappa}_{0\Sigma^+} + (\beta_\Sigma + \beta_\Lambda)\tilde{B}_2 + [\beta_\Sigma(\tilde{e}_{0\Sigma^+} + \tilde{e}_{0\Sigma^0}) + \beta_\Lambda\tilde{e}_{0\Lambda}]\tilde{C}_2 + [\beta_\Sigma(\tilde{\kappa}_{0\Sigma^+} + \tilde{\kappa}_{0\Sigma^0}) + \beta_\Lambda\tilde{\kappa}_{0\Lambda}]\tilde{D}_2\}, \quad (47)$$

$$F_{2\Sigma^0} = Z_\Sigma\{\tilde{\kappa}_{0\Sigma^0} + [\beta_\Sigma(\tilde{e}_{0\Sigma^+} + \tilde{e}_{0\Sigma^-}) + \beta_\Lambda\tilde{e}_{0\Lambda}]\tilde{C}_2 + [\beta_\Sigma(\tilde{\kappa}_{0\Sigma^+} + \tilde{\kappa}_{0\Sigma^-}) + \beta_\Lambda\tilde{\kappa}_{0\Lambda}]\tilde{D}_2\}, \quad (48)$$

$$F_{2\Sigma^-} = Z_\Sigma\{\tilde{\kappa}_{0\Sigma^-} - (\beta_\Sigma + \beta_\Lambda)\tilde{B}_2 + [\beta_\Sigma(\tilde{e}_{0\Sigma^0} + \tilde{e}_{0\Sigma^-}) + \beta_\Lambda\tilde{e}_{0\Lambda}]\tilde{C}_2 + [\beta_\Sigma(\tilde{\kappa}_{0\Sigma^0} + \tilde{\kappa}_{0\Sigma^-}) + \beta_\Lambda\tilde{\kappa}_{0\Lambda}]\tilde{D}_2\}, \quad (49)$$

$$F_{2\Xi^0} = Z_\Sigma\{\tilde{\kappa}_{0\Xi^0} + 2\beta_\Xi\tilde{B}_2 + \beta_\Xi(\tilde{e}_{0\Xi^0} + 2\tilde{e}_{0\Xi^-})\tilde{C}_2 + \beta_\Xi(\tilde{\kappa}_{0\Xi^0} + 2\tilde{\kappa}_{0\Xi^-})\tilde{D}_2\}, \quad (50)$$

$$F_{2\Xi^-} = Z_\Sigma\{\tilde{\kappa}_{0\Xi^-} - 2\beta_\Xi\tilde{B}_2 + \beta_\Xi(2\tilde{e}_{0\Xi^0} + \tilde{e}_{0\Xi^-})\tilde{C}_2 + \beta_\Xi(2\tilde{\kappa}_{0\Xi^0} + \tilde{\kappa}_{0\Xi^-})\tilde{D}_2\}. \quad (51)$$

The magnetic moment of the octet baryon member B is defined in terms of the magnetic form factor $G_{MB} = F_{1B} + F_{2B}$ at $Q^2 = 0$, according to $\mu_B = G_{MB}(0)\frac{e}{2M_B}$. The results for the magnetic moments are usually expressed in terms of the nuclear magneton $\hat{\mu}_N = \frac{e}{2M_N}$, namely, $\mu_B = G_{MB}(0)\frac{M_N}{M_B}\hat{\mu}_N$.

V. PARAMETRIZATIONS

In the previous sections we have defined the general structure of the valence quark part and the functions for the pion cloud. We still need to specify the quark currents in terms of the functions $f_{in}(Q^2)$ ($i = 1, 2$, $n = 0, \pm$), scalar wave functions $\psi_B(P, k)$, and the functions for the pion cloud effects, $\tilde{B}_i$, $\tilde{C}_i$, and $\tilde{D}_i$ ($i = 1, 2$).

A. Parametrization of the quark current

To parametrize the quark current (14), we adopt the structure inspired by the VMD mechanism as in Refs. [1,3],

$$\begin{aligned} f_{1\pm} &= \lambda_q + (1 - \lambda_q)\frac{m_v^2}{m_v^2 + Q^2} + c_\pm\frac{M_h^2Q^2}{(M_h^2 + Q^2)^2}, \\ f_{10} &= \lambda_q + (1 - \lambda_q)\frac{m_\phi^2}{m_\phi^2 + Q^2} + c_0\frac{M_h^2Q^2}{(M_h^2 + Q^2)^2}, \\ f_{2\pm} &= \kappa_\pm\left\{d_\pm\frac{m_v^2}{m_v^2 + Q^2} + (1 - d_\pm)\frac{M_h^2}{M_h^2 + Q^2}\right\}, \\ f_{20} &= \kappa_s\left\{d_0\frac{m_\phi^2}{m_\phi^2 + Q^2} + (1 - d_0)\frac{M_h^2}{M_h^2 + Q^2}\right\}, \end{aligned} \quad (52)$$

where m_v, m_ϕ, and M_h are the masses, respectively, corresponding to the light vector meson $m_v \simeq m_\rho$, the ϕ meson (associated with an $s\bar{s}$ state), and an effective heavy meson with mass $M_h = 2M_N$ to represent the short-range phenomenology. For the isoscalar component it should be $m_v = m_\omega$, but we neglect the small mass difference between the ρ and ω mesons, and use m_ρ. The coefficients c_0, $c_\pm$ and d_0, $d_\pm$ were determined in the previous studies for nucleon (model II) [1] and Ω^- [3]. The values are, respectively, $c_+ = 4.160$, $c_- = 1.160$, $d_+ = d_- = -0.686$, $c_0 = 4.427$, and $d_0 = -1.860$ [3]. The constant $\lambda_q = 1.22$ represents the quark density number in deep inelastic scattering [1].

The isovector $\kappa_+ = 2\kappa_u - \kappa_d$ and isoscalar $\kappa_- = \frac{1}{3}(2\kappa_u + \kappa_d)$ nucleon anomalous magnetic moments were adjusted differently in the past based on the other studies: nucleon elastic form factors [1] or octet baryon magnetic moments [2]. In Ref. [1] the u and d quark anomalous magnetic moments were fixed to describe the nucleon (proton and neutron) magnetic moments using the models without the contributions from the pion cloud at $Q^2 = 0$. More recently, these parameters were updated in a model for the octet baryons with the pion cloud to reproduce the octet baryon magnetic moments [2]. That model was not constrained by the finite Q^2 data, but only by the $Q^2 = 0$ data. In the present study, because we want to describe also the finite Q^2 data, we need to relax the conditions to fix κ_u and κ_d. The quark anomalous magnetic moments will then be constrained by the physical and lattice data. As for κ_s (the strange quark anomalous magnetic moment) it

was fixed as $\kappa_s = 1.462$, to reproduce the Ω^- magnetic moment [3].

The quark form factors parametrized by a VMD mechanism in Eq. (52) are particularly convenient to extend the model to the lattice QCD regime, because they are written in terms of the vector meson and nucleon masses. Then, the extension can be done replacing these masses by those of the lattice regime.

B. Scalar wave functions

Using the expressions (19) and (20), we can determine all the electromagnetic form factors of the octet baryons. To do so, we need to specify the scalar wave functions ψ_B. Generalizing the form used previously for the nucleon [1], we assume the scalar wave functions for the octet baryons in the form

$$\psi_N(P,k) = \frac{N_N}{m_D(\beta_1 + \chi_N)(\beta_2 + \chi_N)}, \tag{53}$$

$$\psi_\Lambda(P,k) = \frac{N_\Lambda}{m_D(\beta_1 + \chi_\Lambda)(\beta_3 + \chi_\Lambda)}, \tag{54}$$

$$\psi_\Sigma(P,k) = \frac{N_\Sigma}{m_D(\beta_1 + \chi_\Sigma)(\beta_3 + \chi_\Sigma)}, \tag{55}$$

$$\psi_\Xi(P,k) = \frac{N_\Xi}{m_D(\beta_1 + \chi_\Xi)(\beta_4 + \chi_\Xi)}, \tag{56}$$

where N_B ($B = N, \Lambda, \Sigma, \Xi$) are the normalization constants, and

$$\chi_B = \frac{(M_B - m_D)^2 - (P-k)^2}{M_B m_D}. \tag{57}$$

Note that, except for the masses, the Λ and Σ scalar wave functions are the same. The normalization constants N_B are determined by

$$\int_k |\psi_B(\bar{P},k)|^2 = 1, \tag{58}$$

where $\bar{P} = (M_B, 0, 0, 0)$ is the baryon four-momentum at its rest frame.

In Eqs. (53)–(56) the parameters β_i ($i = 1, \ldots, 4$) define the momentum range in units of m_D.[1] In the scalar wave functions (53)–(56) with the assumption $\beta_2, \beta_3, \beta_4 > \beta_1$, we associate β_1 with the long-range scale (low momentum range) that is common to all the octet baryon members, and the remaining β_i with the shorter spatial-range scale. The parameters β_1 and β_2 can be determined by the nucleon data only (no strange quarks) in a model without the pion cloud. (See, e.g., Ref. [1].) The parameters β_3 and β_4 are associated with the strange quark. While β_3 is related to the system with one strange quark but β_4 is related to that of the two strange quarks. Since the strange quark is heavier than the u and d quarks, we can expect $\beta_2 > \beta_3 > \beta_4$. The parameters β_i ($i = 1, \ldots, 4$) will be determined later.

[1] In the baryon B rest frame, it reduces to

$$\beta_i + \chi_B = (\beta_i - 2) + 2\frac{E_D}{m_D}.$$

C. Extension of the model for the lattice regime

We now discuss the extension of the model for the lattice regime. In this regime the mass of the octet baryon B is characterized by the pion mass in lattice $m_\pi^{\rm latt}$ and denoted by $M_B^{\rm latt}$. The current j_q^μ [Eq. (14)] is also characterized by the corresponding pion mass in terms of the two components j_1 and j_2, which are represented based on the VMD parametrization in Eq. (52).

In the quark current (14) we replace the coefficient of the Pauli form factor $1/(2M_N)$ by $1/(2M_N^{\rm latt})$ in the lattice regime. As for the quark form factors, we use Eq. (52) with the meson masses replaced by the respective lattice masses as in the previous studies [3,20,33]. Namely, we replace m_v by the lattice ρ mass $m_\rho^{\rm latt}$, and the effective heavy meson mass of $M_h = 2M_N$ by $2M_N^{\rm latt}$. On the other hand, the physical mass is used for m_ϕ, since presently lattice simulations are performed using the physical strange quark mass. To represent the ρ meson mass in the lattice regime, we use the following expression based on the lattice studies made in Ref. [49]:

$$m_\rho^{\rm latt} = a_0 + a_2 (m_\pi^{\rm latt})^2, \tag{59}$$

where $a_0 = 0.766$ GeV and $a_2 = 0.427$ GeV^{-1}. With this procedure we can define unambiguously the quark current.

As for the wave function Ψ_B, M_B is replaced by $M_B^{\rm latt}$ in the lattice regime. This applies for the scalar wave functions (53)–(56). There is no need of modifying the diquark mass in the lattice regime, since the electromagnetic form factors are independent of it. We assume that the range parameters β_i ($i = 1, \ldots, 4$) are independent of the baryon masses and therefore independent of the lattice pion mass $m_\pi^{\rm latt}$. We can expect this approximation to work for a certain range of the $m_\pi^{\rm latt}$ values, but it breaks down for the larger values of $m_\pi^{\rm latt}$ [33].

Using the model extended to the lattice regime, namely, using the quark currents and baryon wave functions in the lattice regime, we can calculate the form factors F_{1B} and F_{2B} in the lattice regime via Eqs. (19) and (20), using the lattice regime masses corresponding to $m_\pi^{\rm latt}$. However, note that the results include only the valence quark contributions, but not the pion cloud contributions.

D. Pion cloud factors

To describe the pion cloud contributions for the octet baryon electromagnetic form factors, we use the following parametrization:

$$\tilde{B}_1 = B_1\left(\frac{\Lambda_{11}^2}{\Lambda_{11}^2 + Q^2}\right)^4, \tag{60}$$

$$\tilde{C}_1 = B_1\left(\frac{\Lambda_{12}^2}{\Lambda_{12}^2 + Q^2}\right)^2, \tag{61}$$

$$\tilde{D}_1 = D_1'\frac{Q^2\Lambda_{13}^4}{(\Lambda_{13}^2 + Q^2)^3}, \tag{62}$$

$$\tilde{B}_2 = B_2\left(\frac{\Lambda_{21}^2}{\Lambda_{21}^2 + Q^2}\right)^5, \tag{63}$$

$$\tilde{C}_2 = C_2\left(\frac{\Lambda_{22}^2}{\Lambda_{22}^2 + Q^2}\right)^3, \tag{64}$$

$$\tilde{D}_2 = D_2\left(\frac{\Lambda_{23}^2}{\Lambda_{23}^2 + Q^2}\right)^3. \tag{65}$$

The parametrization is phenomenological and motivated by the expected falloff of the quark-antiquark contributions at very large Q^2 [50], as well as the magnitude of the pion cloud contributions estimated for the $\gamma N \to \Delta$ reaction [18–20]. The pion cloud contributions should fall off by a factor $1/Q^4$ faster than the falloff of the valence quark contributions. In principle, $\tilde{B}_1$ and $\tilde{B}_2$ should contain the pion electromagnetic form factor $F_\pi(Q^2) \approx (1 + \frac{Q^2}{0.5})^{-1}$, but we adopt simplified functions using just one cutoff parameter with the powers 4 and 5, respectively.

In the above B_1 ($= C_1$), B_2, C_2, and D_2 represent the values of the respective functions at $Q^2 = 0$. The values were determined previously by the octet baryon magnetic moments in Ref. [2]. D_1' is a new constant defined as $D_1' = \frac{1}{\Lambda_{13}^2}\frac{dD_1}{dQ^2}(0)$. However, we do not use the values determined in Ref. [2] in this study. Instead, we will determine them directly by the nucleon form factor data at finite Q^2, and by the Λ, Σ, and Ξ physical magnetic moment data, after determining the contributions from the valence quarks. The adjustable parameters of our pion cloud parametrization are then the coefficients for $Q^2 = 0$, and the cutoffs Λ_{1i} and Λ_{2i} ($i = 1, 2, 3$). But for simplicity, we use and vary only two independent cutoff values for the Dirac and Pauli form factors, respectively, Λ_1 and Λ_2 in this study.

E. Separating the pion cloud contributions

Based on the discussions in the previous sections, the baryon form factors F_{iB} ($i = 1, 2$) may be decomposed into

$$F_{iB}(Q^2) = Z_B[F_{i0B}(Q^2) + \delta F_{iB}(Q^2)], \tag{66}$$

where $F_{10B} = \tilde{e}_{0B}$, $F_{20B} = \tilde{\kappa}_{0B}$, and corresponding $\delta F_{1,2B}$ the pion cloud contributions, which are given in Eqs. (36)–(51). We may regard that $Z_B F_{i0B}$ represent the effects of the valence quarks, and $Z_B\delta F_{iB}$ those of the pion cloud. The same decomposition can be applied for the electric and magnetic form factors

$$G_{EB}(Q^2) = Z_B[G_{E0B}(Q^2) + \delta G_{EB}(Q^2)],$$
$$G_{MB}(Q^2) = Z_B[G_{M0B}(Q^2) + \delta G_{MB}(Q^2)], \tag{67}$$

where $G_{E0B} = \tilde{e}_{0B} - \tau\tilde{\kappa}_{0B}$, $G_{M0B} = \tilde{e}_{0B} + \tilde{\kappa}_{0B}$, $\delta G_{EB} = \delta F_{1B} - \tau\delta F_{2B}$, and $\delta G_{MB} = \delta F_{1B} + \delta F_{2B}$. In this case $Z_B\delta G_{EB}$ and $Z_B\delta G_{MB}$ reflect the dressing of the pion cloud. To estimate the pion cloud contributions, we will compare the full result, G_{EB} or G_{MB}, with the total contributions of the valence quark core, $Z_B G_{E0B}$ or $Z_B G_{M0B}$. The difference is the pion cloud contributions, $Z_B\delta G_{EB}$ or $Z_B\delta G_{MB}$. Hereafter, we will use G_{XB} to express the electric form factor G_{EB} ($X = E$) or the magnetic form factor G_{MB} ($X = M$).

Note that we can alternatively define the contributions from the pion cloud as the difference between the bare form factor, G_{E0B} or G_{M0B}, and the full form factor, G_{EB} or G_{MB}, instead of $Z_B G_{E0B}$ or $Z_B G_{M0B}$ described above. We will refer to these terms as the *effective* pion cloud contributions. By this definition we may have small *effective* pion cloud contributions in the cases, e.g., where $Z_B\delta G_{EB}$ or $Z_B\delta G_{MB}$ are significant.[2] Such an example is the model in Ref. [2]. There the bare contributions for the nucleon magnetic form factor at $Q^2 = 0$, given by $Z_N G_{M0N}$, was about 60% (namely, the pion cloud contributions were $\approx 40\%$), although the *effective* pion cloud contributions were only 5%.

VI. RESULTS

In this section we determine the parameters of the model, and then present results for the valence quark contributions for the octet baryon electromagnetic form factors in the lattice regime, as well as those for the physical regime which includes the pion cloud effects. While the expressions related to the valence quark contributions have been presented in Sec. III D, the formalism related to the pion cloud dressing has been presented in Sec. IV D.

The parameters associated with the valence quark degrees of freedom and the ones associated with the pion cloud dressing are determined by a global fit to the octet baryon electromagnetic form factors, namely, the lattice data, nucleon physical data, and the octet baryon physical magnetic moments. Details are described next. Once we have fixed the relevant parameters, we will discuss the results for the valence quark contributions and the effects of the pion cloud dressing.

[2]The *effective* pion cloud contributions for the form factor G_{XB} are $Z_B\delta G_{XB} - (1 - Z_B)G_{X0B}$. If Z_B differs substantially from 1, the pion cloud contributions $Z_B\delta G_{XB}$ will be modified by the term $-(1 - Z_B)G_{X0B}$, and large cancellation can happen.

A. Global fit

In a regime where the pion cloud effects are small, such as the lattice QCD simulations with heavy pions, or the physical regime at high Q^2, the electromagnetic form factors of the octet baryons should be well described only by the valence quark degrees of freedom. Then, we can use the lattice QCD data with large pion masses to calibrate our model extended to the lattice regime based on the formalism described in Sec. V C, without the pion cloud effects.

To describe the physical octet baryon systems, only the valence quark degrees of freedom are usually insufficient, and explicit pion cloud effects are necessary. Except for the magnetic moments [2], there are no physical data available for the octet baryon form factors besides the nucleon system. Therefore, the nucleon system in the physical regime is ideal to study the pion cloud effects on the form factors at finite Q^2. In this case the nucleon form factors can be described by the mixture of the valence quark and pion cloud contributions given by Eqs. (36), (37), (44), and (45). Also the Λ, $\Sigma^{\pm}$, and $\Xi^{0,-}$ magnetic moments, defined by Eqs. (38)–(43) and (46)–(51) at $Q^2 = 0$, can be used to constrain the effects of the pion cloud at $Q^2 = 0$.

Summarizing, to adjust the parameters of our model, we perform a fit to the lattice data for the valence quark part by extending the model to the lattice regime, and for the pion cloud contributions we perform a fit to the physical data of nucleon form factors and octet baryon magnetic moments. In the latter, the physical regime, the expressions for the form factors are given by extrapolating the bare form factors to the physical case ($m_\pi = 138$ MeV), and the pion cloud contributions are parametrized according to Eqs. (60)–(65). Next, we describe specifically the lattice QCD data and the nucleon physical data. As for the magnetic moments, we use the experimental data for the Λ, $\Sigma^{\pm}$, and $\Xi^{0,-}$ [51]. We do not include the neutron and proton magnetic moments in the fit, since the nucleon magnetic form factor data are also included in our analysis.

1. Lattice data

The lattice data adopted in this work are the octet baryon electromagnetic form factor data from Ref. [52], where n, p, $\Sigma^{\pm}$, $\Xi^{0,-}$ form factors were calculated systematically at finite Q^2 for the first time. The data from Ref. [52] are composed of four sets of unquenched simulations associated with the pion masses 354, 495, 591, and 680 MeV, but restricted to the region $Q^2 < 1.5$ GeV^2. As a total we have 136 data points for both G_{EB} and G_{MB}. To extend our model (valence quark contributions) to the lattice regime, we follow the procedure described in Sec. V C. The relevant variables necessary are the masses associated with the lattice QCD simulations. The corresponding values are presented in Table IV according to the simulations of Ref. [52], and the m_ρ values determined through Eq. (59).

TABLE IV. Masses of the octet baryons (M_N, M_Σ and M_Ξ) obtained in lattice QCD in Ref. [52]. The ρ meson mass is obtained using the parametrization (59). The first row corresponds to the physical values. In the physical case it is also $M_\Lambda = 1.116$ GeV.

m_π(GeV)	m_ρ(GeV)	M_N(GeV)	M_Σ(GeV)	M_Ξ(GeV)
0.138	0.779	0.939	1.192	1.318
0.351	0.820	1.150	1.349	1.438
0.495	0.871	1.290	1.410	1.475
0.591	0.915	1.366	1.448	1.491
0.690	0.964	1.490	1.524	1.546

2. Nucleon physical data

For the nucleon we have included the proton electric and magnetic form factors (G_{Ep} and G_{Mp}), and neutron electric and magnetic form factors (G_{En} and G_{Mn}). Since one of our goals in this work is to describe the octet baryon lattice data for G_{EB} and G_{MB}, we do not adopt the ratio G_{EB}/G_{MB}, although it is considered in many studies of the proton electromagnetic form factors.

The proton data can be extracted using the *classical* Rosenbluth separation technique from the cross section data, or the polarization transfer method developed at Jefferson Lab to measure the ratio G_{Ep}/G_{Mp} [53,54]. The results of the two methods show discrepancies that can possibly be explained by including the two-photon exchange corrections in the results of the Rosenbluth separation method [17,55]. An analysis that takes into account the two-photon exchange corrections and uses the cross section information to determine the values of G_{Ep} and G_{Mp} separately (not just the ratio) was presented in Ref. [55]. Since our calculations are performed in the impulse approximation, we compare our results with the analysis of Arrington *et al.* [55], where the two-photon exchange contributions were subtracted. To include the recent, high Q^2 results for G_{Ep}/G_{Mp} from Jefferson Lab [54], we convert the ratio G_{Ep}/G_{Mp} into G_{Ep} using the fit to the G_{Mp} presented in Ref. [55]. The fit is accurate for a large Q^2 range ($Q^2 = 0$–10 GeV^2). Overall, we have 50 data points for G_{Ep} and 56 data points for G_{Mp}.

As for the neutron form factors, we collect the data from different groups. We prefer to use the data extracted from a deuterium target rather than those extracted from a ^{3}He target, since the former is expected to have fewer nuclear corrections. For G_{En} we use the data from Mainz [56], NIKHEF [57], MIT-Bates [58], and Jefferson Lab [59,60]. The results from Ref. [60] obtained using the ^{3}He target, corresponding to the highest Q^2 result for G_{En} ($Q^2 = 3.4$ GeV^2), are also included. Also the results obtained from the deuteron electric quadrupole moment are included [61]. For G_{Mn} we adopt the data used by Bosted *et al.* [62] in the global fit of the nucleon data, as well as more recent data from Mainz [63] and Jefferson Lab [64].

Totally, we have 29 data points for G_{En} and 67 data points for G_{Mn}.

The inclusion of the high Q^2 region nucleon data, where pion cloud effects are expected to be small, is important for the calibration of our model in the valence quark sector, since the information of lattice simulations is restricted to the low Q^2 region. We can test the parametrization directly by the nucleon elastic form factor data that are extended for the proton up to 9 and 31 GeV^2, respectively, for G_{Ep} and G_{Mp}, and for the neutron up to 3.4 and 10 GeV^2, respectively, for G_{En} and G_{Mn}.

3. Details of the fit

The parameters associated with the valence quark contributions are adjusted to the lattice data (bare form factors), the bare part of the nucleon form factors at the physical point, and octet baryon magnetic moments. They are the momentum-range parameters of the scalar wave functions, β_i ($i = 1, \ldots, 4$), and the u and d quark anomalous magnetic moments κ_u and κ_d, respectively. The strange quark anomalous magnetic moment κ_s is kept unchanged, since it was fixed by the Ω^- magnetic moment, which is not affected by the pion cloud [3].

The pion cloud contributions are adjusted by the nucleon physical data and the octet baryon magnetic moment data. We start by calculating the bare form factors $\tilde{e}_{0B}$ and $\tilde{\kappa}_{0B}$ at the physical point ($m_\pi = 138$ MeV), using only the parametrization for the bare form factors. Next, we add for each form factor, F_1 and F_2, or alternatively G_E and G_M, the pion cloud contributions given by Eqs. (60)–(65). For this, we need to fix the parameters B_1, B_2, C_1, D_1', D_2 and the cutoffs Λ_1 and Λ_2. These parameters are adjusted by the nucleon form factor data for G_E and G_M, and octet baryon magnetic moments, since the magnetic moments are proportional to $G_{MB}(0)$. In the latter we have additional constraints for the coefficients B_1, C_1, C_2, and D_2 [2]. (The calibration of D_1', Λ_1 and Λ_2 can be done only with $Q^2 > 0$ data). Once we have fixed the parameters associated with the pion cloud, we can obtain explicit expressions for the pion cloud contributions for the octet baryon electromagnetic form factors.

For very large pion masses, it is not reasonable to assume the baryon wave functions can be described by the same parameters, but some dependence on the baryon masses (indirect dependence on the quark mass) may enter. Also, for small pion masses ($m_\pi < 400$ MeV) one can expect that lattice simulations may be affected by the pion cloud effects, and as a consequence form factor data should differ from the calculation based solely on the valence quark degrees of freedom. The ideal situation would be to use several sets of lattice data in the region 400 MeV $< m_\pi <$ 600 MeV. In this way we expect to avoid both the pion cloud contamination, and the very large m_π region where the model can fail. In the previous studies, this way of extension to the lattice regime was very successful [20,33].

A preliminary analysis of the lattice data has revealed that the set $m_\pi = 591$ MeV is particularly difficult to describe in our model (large χ^2 per data point as presented in Table V), although the quality of the fit is improved for the next set[3] ($m_\pi = 691$ MeV). Using efficiently the available lattice QCD data for the octet baryon electromagnetic form factors, and at the same time to keep a reasonable description of the present model, we perform a fit to the first two sets of lattice data, $m_\pi = 351$ and 495 MeV. (The risk of the pion cloud contamination in the $m_\pi = 351$ MeV set is compensated by the increase of accuracy in the set.)

Another point to be noted in our analysis is the lattice data for the neutral particles, n and Ξ^0. The results for the n and Ξ^0 electric charge form factors at $Q^2 = 0$ (their charges) differ from zero, and this fact suggests that the lattice results have some systematic errors. This may be a consequence of incomplete cancellations among the contributions from the different quark flavors for the form factors [52], and we have to take this into account. In order to use the n and Ξ^0 data but achieve a reasonable accuracy, we reduce the respective impact on χ^2 by doubling the respective statistical errors.

As already mentioned, the pion cloud parametrization is calibrated using the Λ, $\Sigma^\pm$, $\Xi^{0,-}$ physical magnetic moment data and the nucleon physical data. Some of the octet magnetic moment data are extremely accurate with error bars of less than 1% (Λ and Σ^-). A minimization of χ^2 with such small error bars of $G_{MB}(0)$ will impose strong contributions on χ^2 in the $Q^2 = 0$ region, and reduce the relative impact of the region $Q^2 > 0$, represented by the nucleon form factor data. To achieve a good description (low χ^2/n_p, where n_p is the number of the data points) for the nucleon data, we reduce the weight of the octet baryon magnetic moment data, by doubling the experimental errors.

We define the best model as the model that minimizes the total χ^2 associated with the lattice data, the octet magnetic moment data, and nucleon physical data as described before. Totally, we have 272 lattice data points, 5 experimental magnetic moment data points, and 202 nucleon physical data points.

A fit with no constraints leads to a good description of the lattice data (small χ^2 per data point), but a poor description of the nucleon physical data with χ^2 per data point >2. That fit generates also a large contributions from the pion cloud effects, and has a large extension in Q^2 from the pion cloud effects, in particular, for G_M due to a large cutoff Λ_2 compared to 1 GeV. We interpret this result as a consequence of the dimension of the lattice database (272 data points) for 6 baryons including the nucleon, to be

[3]Although the quality of a global fit is measured by the total χ^2 divided by [(the number of data points) − (the number of parameters)] considered in the fit, to estimate the quality of the subsets of data, it is simpler to ignore the subtraction of the number of parameters, since the parameters are not fixed by one subset of the data.

TABLE V. χ^2 decomposition of the best fit to the lattice data and nucleon physical data. The numbers in the rows corresponding to $m_\pi = 138$ MeV (nucleon data) include the effects of the pion cloud. See also the discussion in the text. For the lattice data, χ^2 per data point is 5.00 (2.93 excluding the n and Ξ^0 data).

m_π(MeV)	p	n	Σ^+	Σ^-	Ξ^0	Ξ^-	χ^2
354	0.244	3.025	4.841	1.891	19.197	0.121	1.768
	1.729	4.872	7.197	0.350	38.909	6.101	4.063
	0.987	3.948	6.019	1.120	29.053	3.111	**2.915**
495	0.557	1.790	1.254	17.313	78.699	14.361	8.014
	2.612	7.696	5.200	1.448	25.125	1.340	2.440
	1.585	4.743	3.227	9.381	51.912	7.850	**5.227**
591	21.297	19.267	8.332	16.865	156.552	9.733	14.057
	13.540	34.159	24.882	5.558	37.069	12.414	14.099
	17.418	26.713	16.607	11.212	96.810	11.073	14.078
680	13.219	22.808	3.116	2.994	115.990	8.981	7.077
	4.079	13.787	5.265	0.067	9.063	3.682	3.273
	8.649	18.297	4.190	1.530	62.526	6.332	5.175
138	1.600	1.872					1.700
	1.857	2.273					2.083
	1.736	2.152					**1.933**

compared with the nucleon physical data (202 data points). This procedure reduces the relative importance of the nucleon physical data. Since we want to describe well the nucleon system but simultaneously to have a reasonable description of the lattice data, we reinforce the impact of the nucleon physical data by doubling the contributions of their χ^2 in the global evaluation of χ^2. The fit with this constraint leads a good qualitative description of the nucleon physical data (χ^2 per data point $\simeq 1.9$), and also reasonable values for the cutoffs Λ_1 and Λ_2, where the values are smaller than 1 GeV, or closer to 1 GeV, consistent with the pion cloud effects restricted to low Q^2 region. The values of the cutoffs will be discussed in more detail later. As we will see, the final fit is consistent with the small pion cloud contributions for the octet baryon form factors.

The quality of the fit, measured in terms of χ^2 per data point, can be understood from Table V. In the table we represent for each set, $\chi^2(G_{EB})$ in the first row, $\chi^2(G_{MB})$ in the second row, and the combined result in the last row. In boldface we represent the χ^2 for the sets considered in the fit. The rows associated with the physical regime ($m_\pi = 138$ MeV) are the only ones that reflect the effects of the pion cloud. Note that the sets $m_\pi = 591$ and 680 MeV are not included in our fit. In the last column we represent the partial $\chi^2(G_E)$ and $\chi^2(G_M)$, and the total χ^2, associated with respective sets. In this case the contributions from n and Ξ^0 are not included.

B. Bare octet form factors

The results of the fit for the octet baryon electromagnetic form factors are presented in Figs. 3–10. The values of the pion mass in the fit are $m_\pi = 354$ and 495 MeV. For the nucleon [Figs. 3 and 4], we present also the physical case ($m_\pi = 138$ MeV). The parameters associated with the results are

$$\beta_1 = 0.0440, \quad \beta_2 = 0.9077, \quad \beta_3 = 0.7634,$$
$$\beta_4 = 0.4993, \quad \kappa_u = 1.6690, \quad \kappa_d = 1.9287. \tag{68}$$

We note that the (bare) quark anomalous magnetic moments, κ_u and κ_d, are similar to the previous results obtained in Refs. [1,2], within a 16% variation. (In Refs. [1,3] the values obtained are $\kappa_u = 1.778$ and $\kappa_d = 1.915$, while in Ref. [2] they are $\kappa_u = 1.929$ and $\kappa_d = 1.919$.)

Furthermore, the values for β_1 and β_2 are also similar to those of the model in Ref. [1] ($\beta_1 = 0.049$ and $\beta_2 = 0.717$). Interpreting β_1 as the spatial long-range parameter common to all the systems associated with one light quark (N, Σ, Λ, and Ξ), β_2, β_3, and β_4 are interpreted as spatial short-range parameters associated with spatial extension of the $q_l q_l$, $q_l s$, and ss quark pairs, respectively, where q_l stands for a light quark. In this respect we should expect $\beta_2 > \beta_3 > \beta_4$, as observed, consistently with Eq. (68), a decreasing of the spatial extension of the systems, gradually from the nucleon followed by the Λ, Σ, and finally by the Ξ system. The systems with one strange quark are more compact than the ones with no strange quarks, and the systems with two strange quarks are even more compact than the ones with only one strange quark. We will return to this issue later when we discuss the charge and magnetic squared radii.

In Figs. 3–10 we compare the results of our fit for the n, p, Λ, $\Sigma^{0,\pm}$, and $\Xi^{0,-}$ with the lattice data for $m_\pi = 354$ and 495 MeV. The lattice data [52] used in the fit are shown

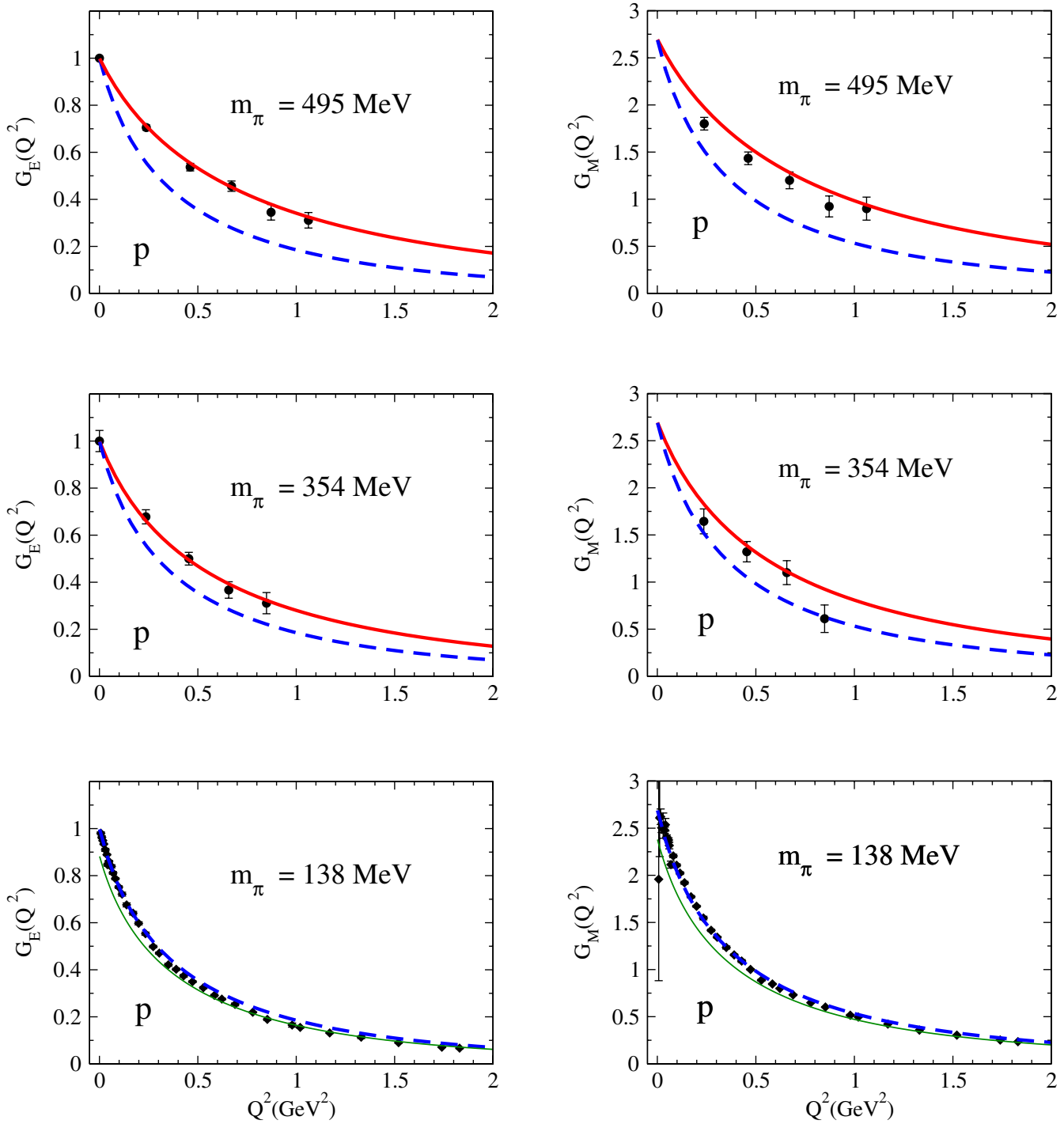

FIG. 3 (color online). Bare electromagnetic form factors for the proton determined by the global fit, compared with the lattice data from Ref. [52]. The lines are the lattice regime (solid line) and the physical regime (dashed line). For $m_\pi = 138$ MeV, we include the physical data. The thin solid lines in the bottom panels do not include the pion cloud contributions.

in Figs. 3, 4, 6, and 8–10, respectively, for the p, n, Σ^+, Σ^-, Ξ^0, and Ξ^-. For the proton and neutron we include also the physical case ($m_\pi = 138$ MeV) and compare the results with the experimental data (details will be discussed later). We have no data for the Λ and Σ^0 from Ref. [52], respectively, shown in Figs. 5 and 7, but we compare our results with the quenched lattice QCD simulation results from Ref. [65] with the closest pion mass values, respectively $m_\pi = 372$ and 464 MeV, for the single point at $Q^2 = 0.23$ GeV^2 calculated in that work.

Overall, we have a very good description of the data for p, $\Sigma^\pm$ and even Ξ^-. As mentioned already, the results for n and Ξ^0 should be taken with caution, since the lattice simulations have systematic deviations from the expected

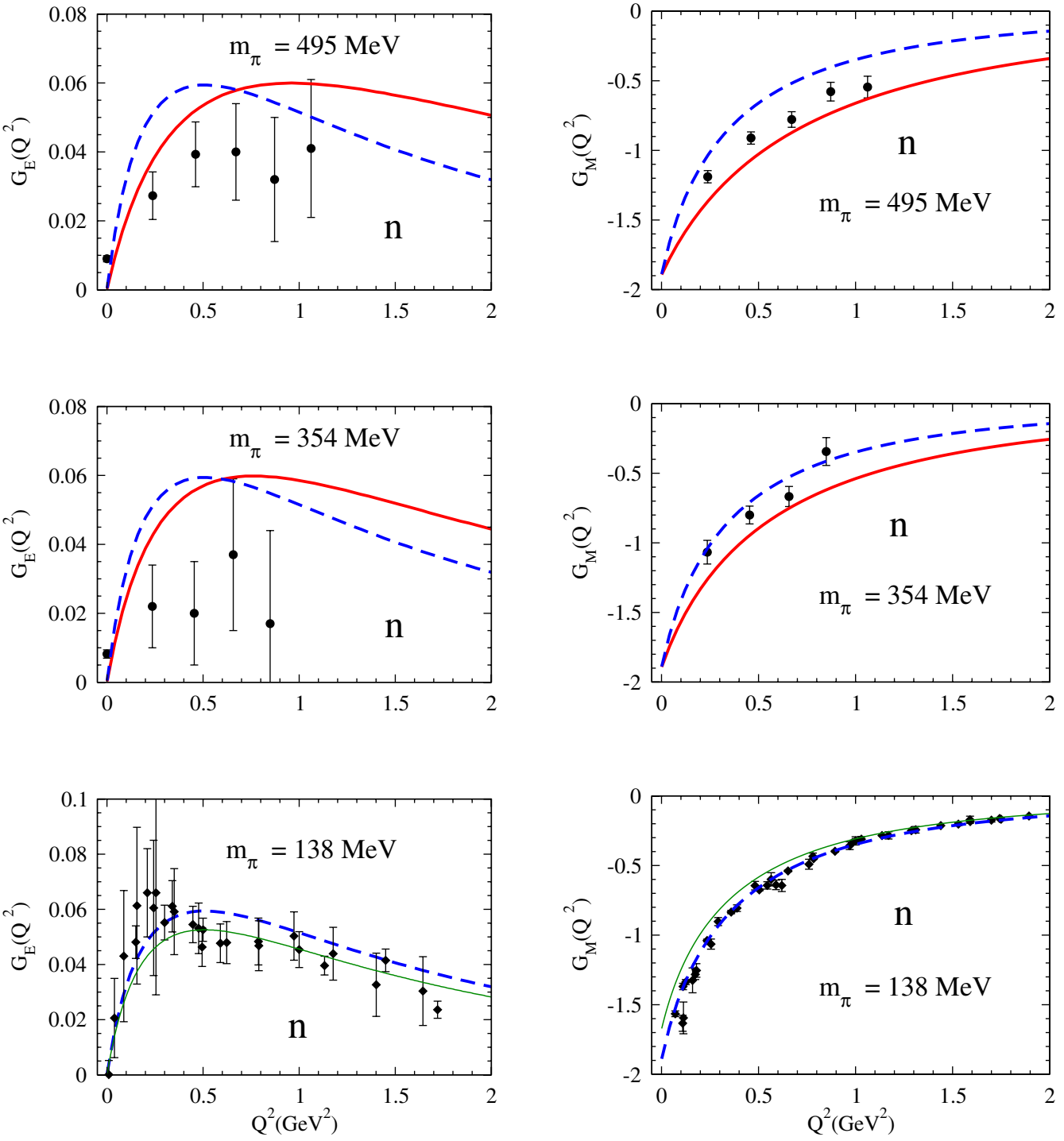

FIG. 4 (color online). Bare electromagnetic form factors for the neutron determined by the global fit, compared with the lattice data from Ref. [52]. The lines are the lattice regime (solid line) and the physical regime (dashed line). For $m_\pi = 138$ MeV, we include the physical data. The thin solid lines in the bottom panels do not include the pion cloud contributions.

results, particularly for the electric charge form factors. Nevertheless, we have a good global description of the nucleon and Σ systems. As for the Ξ, the lattice results are closer to the extrapolation to the physical limit (dashed line) than the calculation in the lattice regime (solid line). This can be caused by the poor quality of the G_E data for Ξ^0 as discussed before, or a limitation of our simplified approach. Further lattice QCD simulation data, consistent with the n and Ξ^0 charges, are necessary to clarify this point. As for the other neutral particles, Λ and Σ^0, our predictions are consistent with the simulations of Boinepalli *et al.* [65], within about 2 standard deviations,

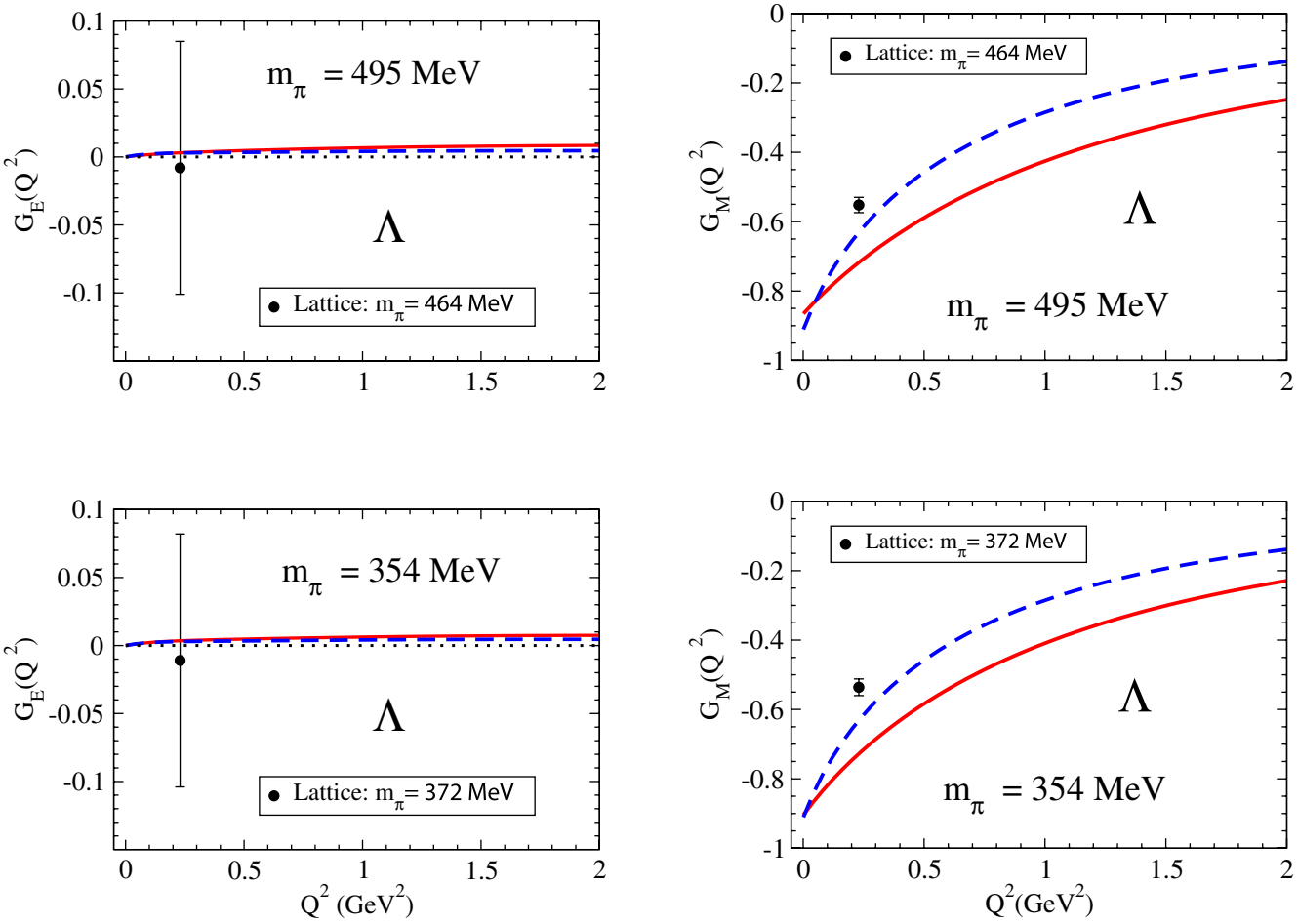

FIG. 5 (color online). Λ bare electromagnetic form factors determined by the global fit. The lines are the lattice regime (solid line) and the physical regime (dashed line). For the lattice regime calculations, we use the value $M_\Lambda = M_\Sigma$, where M_Σ is the Σ mass from Table IV. For the physical point we use the physical Λ mass. The lattice data are from Ref. [65] for $m_\pi = 372$ and 464 MeV.

for the closest pion mass values used. A final remark is on the difficulty of the present approach in describing the n and Ξ^0 data. Since we try to describe well F_1 and F_2 (or G_E and G_M) simultaneously, inaccuracy in one set (say G_E) will affect the description of the other set (say G_M).

For the nucleon system we compare also the results extrapolated to the physical limit of the bare form factors with the physical data [see the bottom panels with $m_\pi = 138$ MeV in Figs. 3 and 4]. Note that these results should not be compared directly, since we have not yet included the pion cloud effects in the calculation. From the figures, our aim is to see whether or not the pion cloud effects are indeed important, and if a reasonable description of the data can be achieved without the pion cloud effects. We plot then the results of two different calculations. The first one is the extrapolation to the physical limit of the model, represented by the dashed line (the same as in the upper panels). The result is obtained setting $Z_N = 1$, in the expression for the nucleon form factors [Eqs. (36), (37), (44), and (45)], and removing the pion cloud contributions. Plotted in the same figures (thin solid line) is the same calculation but for the case $Z_N = 0.885$, given by the fit, the contributions exclusively from the valence quark core. From the results shown in the figures, we conclude that the data are well described by a model with no pion cloud effects, although in the region of high Q^2 (say $Q^2 > 1$ GeV^2), the model with $Z_N = 0.885$ given by the thin solid lines (solely from the valence quark contributions), are closer to the data than those of $Z_N = 1$.

C. Pion cloud contributions

We discuss now the calibration of the pion cloud effects. The values in the parametrization associated with the pion cloud effects are

$$B_1 = 0.04343, \quad B_2 = 0.21477, \quad C_2 = 0.02266,$$
$$D_1' = -0.17637, \quad D_2 = 0.08551, \tag{69}$$

with the cutoff values,

$$\Lambda_1 = 0.7732 \text{ GeV}, \quad \Lambda_2 = 1.2455 \text{ GeV}. \tag{70}$$

The quality of the fit associated with the pion cloud effects is measured by the partial χ^2 values for the nucleon

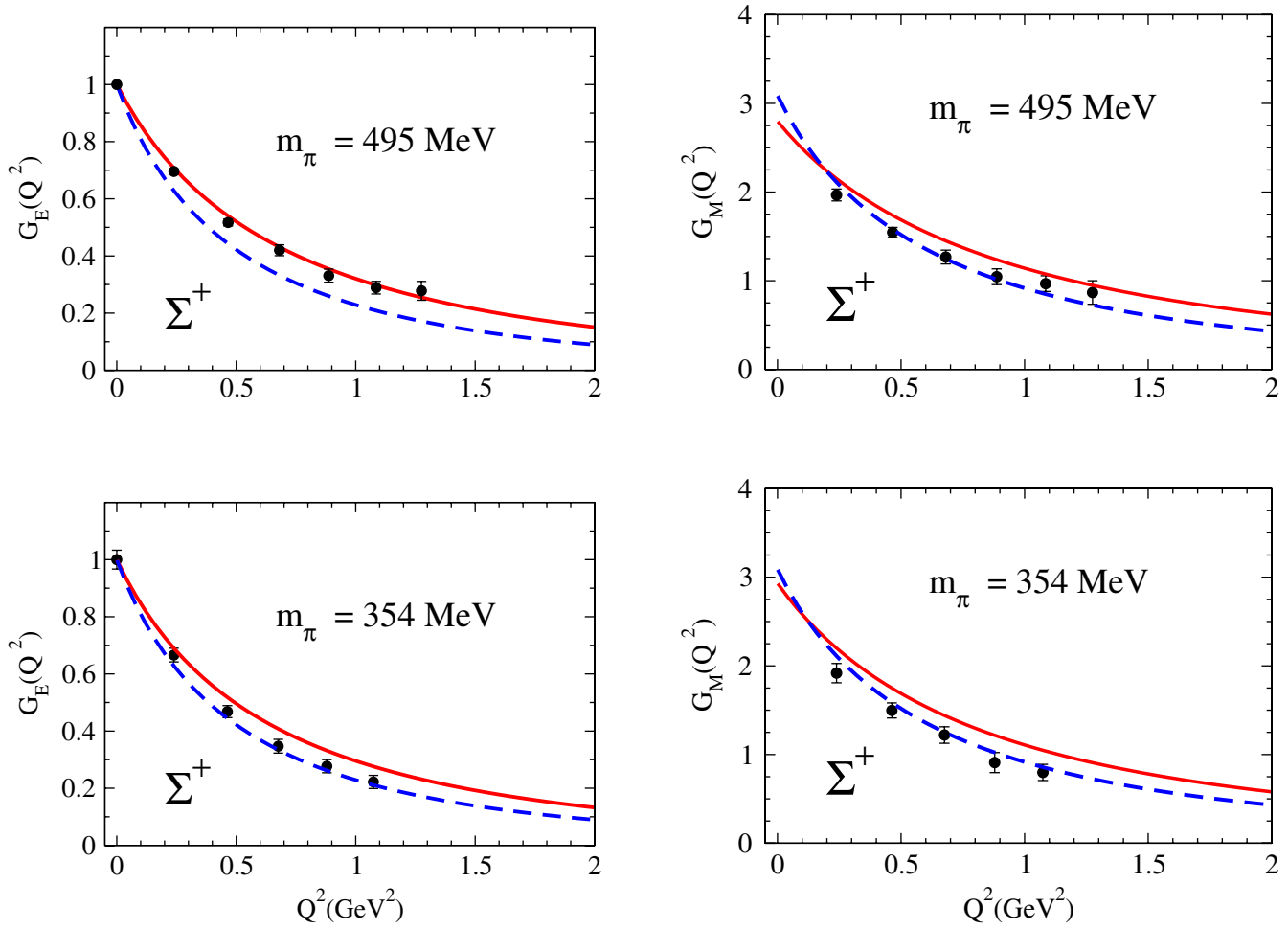

FIG. 6 (color online). Σ^+ bare electromagnetic form factors determined by the global fit. The lines are the lattice regime (solid line) and the physical regime (dashed line). The lattice data are from Ref. [52].

system at the physical point, given by the last column in Table V (χ^2 per data point = 1.93). Then, we can conclude that the nucleon data are described better than the lattice data (χ^2 per data point of 2.9 and 5.2 for the sets $m_\pi = 354$ and 495 MeV, respectively).

Since we cannot isolate the pion cloud contributions from the valence quark contributions in the experimental data, we analyze the pion cloud effects by comparing the individual components of the nucleon form factors with the full result. The results for the nucleon are presented in Fig. 11, where the form factors are renormalized by the dipole form factor $G_D = (1 + \frac{Q^2}{0.71})^{-2}$. The exception is the neutron electric form factor. In the figure, the contributions of the pion cloud are represented by the bands that fill the difference between the valence quark contributions ($Z_B G_{X0B}$) and the full result (G_{XB}, solid line).

Observing the pion cloud contributions for the nucleon electromagnetic form factors in Fig. 11, we conclude that the contributions are similar for both the proton and neutron magnetic form factors. In both cases contributions amount to 10–14% in the region of $Q^2 = 0$–0.5 GeV^2, and fall to less than 5% around $Q^2 = 2$ GeV^2, and even become less than 1% for $Q^2 > 5$ GeV^2.

The analysis for the electric form factors is more delicate. For the proton there are $\approx 12\%$ contributions from the pion cloud near $Q^2 = 0$, and they fall to 1% near $Q^2 = 1$ GeV^2, and stabilize to 5% negative contributions for $Q^2 \approx 5$ GeV^2. In the larger Q^2 region one must be careful, since G_E approaches zero and the ratio is not meaningful. For $Q^2 = 10$ GeV^2 the valence quark contributions are larger than 90%. As for the neutron near $Q^2 = 0$, where $G_{En}(0) = 0$, the pion cloud contributions dominate. Near $Q^2 = 1$ GeV^2, the pion cloud effects are about 10% and drop to less than 4% for $Q^2 = 4$ GeV^2, and even smaller for larger Q^2. For $Q^2 = 10$ GeV^2 the valence quark contributions dominate to give more than 98%.

The slow falloff of the pion cloud contributions for the electric form factors compared with those for the magnetic ones is due to the enhancement of the F_2 contributions for G_E by the prefactor Q^2, and the function form for the pion cloud contributions. Since the pion cloud contributions are regulated by the cutoff $\Lambda_2 = 1.24$ GeV

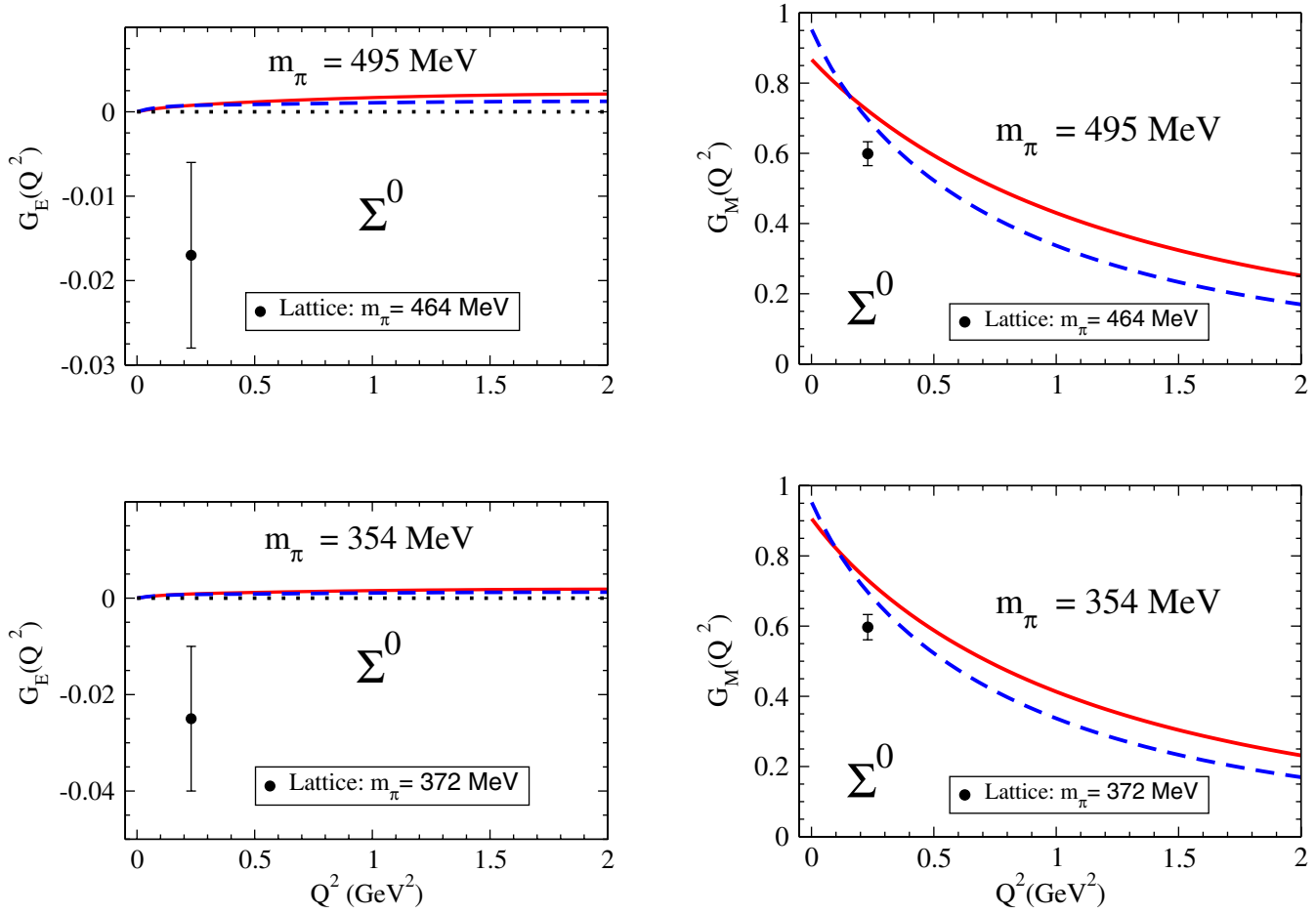

FIG. 7 (color online). Σ^0 bare electromagnetic form factors determined by the global fit. The lines are the lattice regime (solid line) and the physical regime (dashed line). The lattice data are from Ref. [65] for $m_\pi = 372$ and 464 MeV.

($\Lambda_2^2 = 1.55$ GeV^2), which is larger than $\Lambda_1 \simeq 0.77$ GeV ($\Lambda_1^2 = 0.59$ GeV^2), the electric form factor is extended to the higher Q^2 region due to the range of the pion cloud contributions in F_2.

We point out the qualitative differences of the pion cloud contributions between the present results and those of the previous study in the octet baryon magnetic moments [2]. In the previous study the Q^2 dependence was not taken into account (no use of lattice data or the nucleon physical form factor data), and the pion cloud contributions were significantly larger. Thus, we can conclude that the Q^2 dependence of the pion cloud contributions is very important to constrain the pion cloud contributions, in particular, for the nucleon system.

D. Dressed form factors

Taking into account the results for the bare form factors extracted from the lattice data, and the pion cloud parametrization from the previous section, we use the expressions in Sec. IV D to predict the dressed, physical form factors for the Λ, Σ, and Ξ systems in the physical regime ($m_\pi = 138$ MeV). The predicted results are presented in Figs. 12–14. In the figures we show the full results (solid line) and bare results (dashed line). Included in the figures are also the magnetic moments when known (Λ, $\Sigma^\pm$, and $\Xi^{0,-}$). To have an idea for the dynamical behavior (Q^2 dependence) of the form factors, we include also the lattice QCD simulation data corresponding to the lowest pion mass from Ref. [65] ($m_\pi = 306$ MeV). In principle, the lattice data should be compared with the bare form factors (dashed line), unless strong quenched effects are expected.

An important conclusion from the figures is that the magnitude of the pion cloud contributions is small. Based on the magnetic moments, we have more significant contributions from the pion cloud for Σ^-, Σ^+, and Λ, respectively, about 21%, 14%, and 14%, and less than 10% for all other cases. With the exception of the neutral particles Λ, Σ^0, and Ξ^0, where pion cloud effects can be dominant, the pion cloud contributions for the electric form factors are smaller than those for the magnetic form factors.

Overall, our predictions for the octet baryon electromagnetic form factors, as functions of Q^2, are consistent with the results for the magnetic moments (at $Q^2 = 0$), and close to the lattice QCD simulations. The major exception is the results for Ξ^0, where we observe the clear deviation

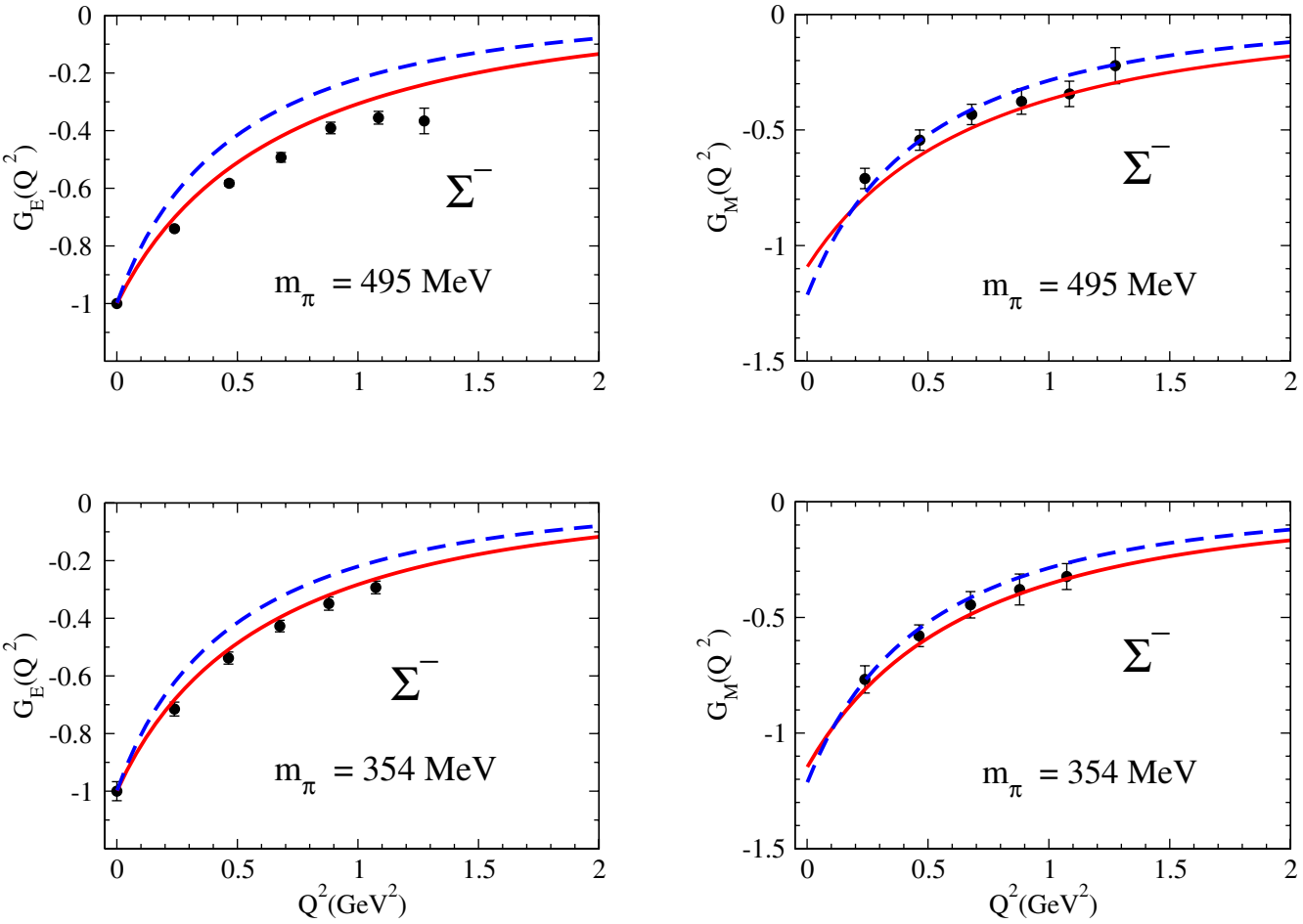

FIG. 8 (color online). Σ^- bare electromagnetic form factors determined by the global fit. The lines are the lattice regime (solid line) and the physical regime (dashed line). The lattice data are from Ref. [52].

from the experimental result for $G_M(0)$, and also from the lattice data. We recall again that this can be a consequence of the difficulty in describing the Ξ lattice data. [See Figs. 9 and 10.]

E. Electric charge and magnetic dipole radii

The electric charge squared radius for a charged particle is usually defined as[4]

$$\langle r_E^2 \rangle = -\frac{6}{G_{EB}(0)} \frac{dG_{EB}}{dQ^2}\bigg|_{Q^2=0}. \tag{71}$$

For a neutral particle the same expression can be used but setting $G_{EB}(0) \to 1$. The definition (71) has advantages for comparing the radii of particles with different charges such as p and Σ^-, and one can relate the corresponding baryon electric charge radii. As for the magnetic dipole squared radius, the most common definition[5] is

$$\langle r_M^2 \rangle = -\frac{6}{G_{MB}(0)} \frac{dG_{MB}}{dQ^2}\bigg|_{Q^2=0}. \tag{72}$$

We assume in this case that $G_{MB}(0)$ is not zero, neither very small. The results for the electric charge squared radii and the magnetic squared radii are, respectively, presented in Tables VI and VII (see columns $\langle r_E^2 \rangle$ and $\langle r_M^2 \rangle$). Experimental values [51,66–71] are also included in Table VI for $\langle r_E^2 \rangle$, and in the caption of Table VII for $\langle r_M^2 \rangle$.

Since in the present approach we can identify the valence quark (bare) contributions and the pion cloud contributions in the form factor G_{XB} ($X = E, M$), we follow Eq. (67) and decompose G_{XB} into

$$G_{XB}(Q^2) = G_{XB}^b(Q^2) + G_{XB}^\pi(Q^2), \tag{73}$$

where $G_{XB}^b(Q^2) = Z_B G_{X0B}(Q^2)$ and $G_{XB}^\pi(Q^2) = Z_B \delta G_{XB}(Q^2)$, are, respectively, the bare and pion cloud contributions. Based on the decomposition (73) and the definitions of radii (71) and (72), we can write

$$\langle r_E^2 \rangle = \langle r_E^2 \rangle_b + \langle r_E^2 \rangle_\pi, \tag{74}$$

$$\langle r_M^2 \rangle = \langle r_M^2 \rangle_b + \langle r_M^2 \rangle_\pi, \tag{75}$$

[4]Some authors [65] exclude the factor $G_{EB}(0)$ from the $\langle r_E^2 \rangle$ definition.

[5]Some authors [65] define $\langle r_M^2 \rangle$ without the factor $G_{MB}(0)$, but use $\frac{\langle r_M^2 \rangle}{G_{MB}(0)}$ to compare the values of different baryons.

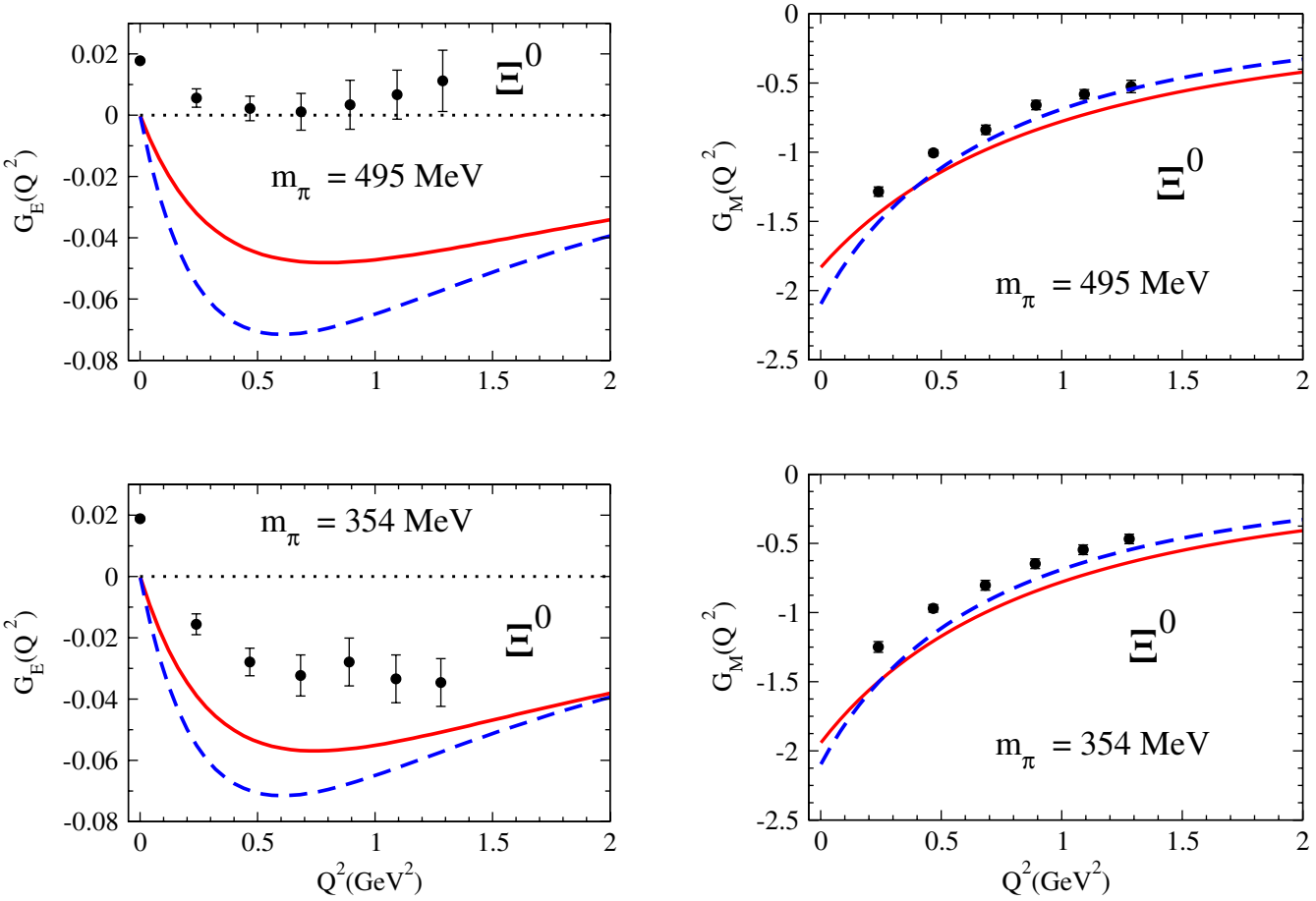

FIG. 9 (color online). Ξ^0 bare electromagnetic form factors determined by the global fit. The lines are for the lattice regime (solid line) and the physical regime (dashed line). The lattice data are from Ref. [52].

where

$$\langle r_E^2\rangle_b = -Z_B \frac{6}{G_{EB}(0)} \frac{dG_{E0B}}{dQ^2}\bigg|_{Q^2=0}, \tag{76}$$

$$\langle r_M^2\rangle_b = -Z_B \frac{6}{G_{MB}(0)} \frac{dG_{M0B}}{dQ^2}\bigg|_{Q^2=0}, \tag{77}$$

and $\langle r_E^2\rangle_\pi$ and $\langle r_M^2\rangle_\pi$ can be defined in a similar manner, but using $\delta G_{EB}(Q^2)$ and $\delta G_{MB}(Q^2)$, or from Eqs. (74) and (75), by subtracting the bare components from the total.

Since our form factors are determined numerically, we calculate the octet baryon electric charge squared radii and magnetic dipole squared radii, as well as the respective components, using numerical derivatives. The contribution from each component is also presented in Tables VI and VII.

From the global results for $\langle r_E^2\rangle$ and $\langle r_M^2\rangle$, we can conclude that the nucleon system has larger spatial charge and magnetization distributions than that of the Σ system, and that the Σ system has the larger spatial charge and magnetization distributions than those of the Ξ system. We will leave the neutral particles (n, Λ, Σ^0, and Ξ^0) out of the discussion for $\langle r_E^2\rangle$. Our results suggest that the electric charge squared radii of 0.7–0.8 fm^2 for proton (p), 0.6–0.7 fm^2 for $\Sigma^\pm$, and 0.4 fm^2 for Ξ^-. These results may support the general idea that the systems with two strange quarks (Ξ) are more compact than the systems with only one strange quark (like Σ), and the latter systems are more compact than the nucleon in charge density distributions. The statement becomes more clear when we look at the magnetic squared radii, where we have now 0.7 fm^2 for N, 0.5–0.6 fm^2 for Σ, and 0.3–0.4 fm^2 for Ξ. Note that, for $\langle r_M^2\rangle$, the magnitudes hold also for the neutral particles.

Our results for $\langle r_E^2\rangle$ are compared in Table VI with the experimental results for p, n, and Σ^-. With the exception for the neutron, to be discussed later, our results are consistent with the experimental values. We compare also our results with the estimates from Ref. [31]. In that work the octet baryon electric charge radii were extrapolated from the quenched lattice QCD data [65] to the physical point using chiral perturbation theory, including corrections for both the finite volume and quenched effects. Aside from Λ and Σ^0 which were not estimated (and n to be discussed latter), the results of Ref. [31] are in agreement with our results. We recall that Λ (like Σ^0) has not been included in the calibration of our model, since the properties of Λ were

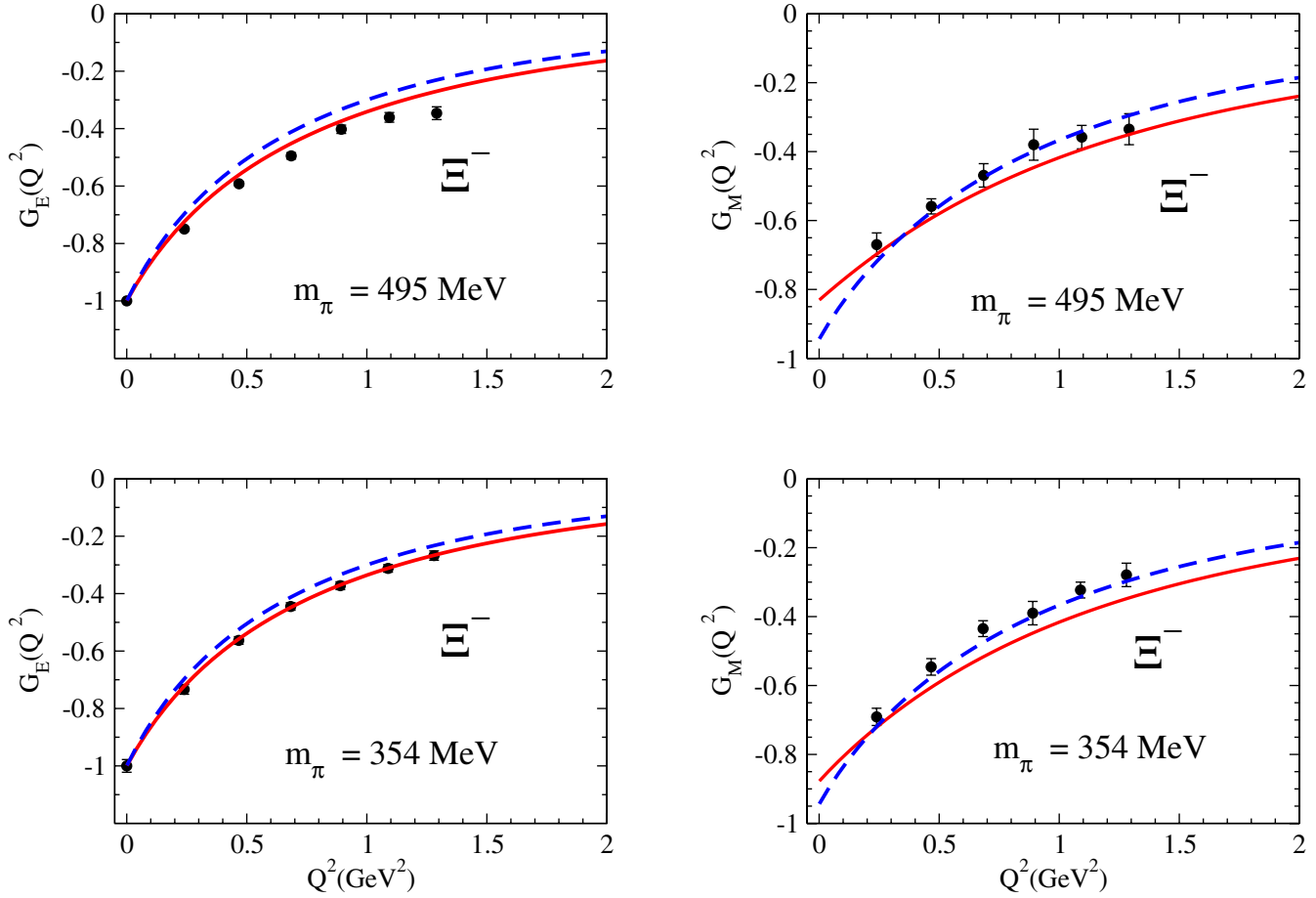

FIG. 10 (color online). Ξ^- bare electromagnetic form factors determined by the global fit. The lines are the lattice regime (solid line) and the physical regime (dashed line). The lattice data are from Ref. [52].

not calculated in the lattice simulations in Ref. [52], on which our parametrization is based. Note however, our result for the Λ electric charge squared radius is also very small (0.08 fm^2), although larger than the result of Ref. [65], 0.003–0.017 fm^2. We recall again that the electric charge form factors of neutral particles are difficult to simulate in lattice QCD, due to the cancellation among the contributions from the different flavor quarks, which should cancel out exactly at $Q^2 = 0$. Our results can also be compared with other estimates presented in the literature [11,12,24,72–79].

Using the decompositions of Eqs. (74) and (75), we separate also the effects of the valence quarks and those of the pion cloud. The results decomposed for $\langle r_E^2 \rangle$ are presented in the second and third columns in Table VI. Focusing first on the charged baryons, the valence quarks give dominant contributions, although the pion cloud effects can be important and as large as 33% for the Σ^+. Since the effective contributions of the valence quarks were also estimated in Ref. [31], we compare $\langle r_E^2 \rangle_b$ directly with those results (third column) in Table VIII. Although the meson cloud contributions in Ref. [31] are not the same as ours, and also kaon cloud contributions are included (but amounted to small contributions), it can be illustrative to compare our results of $\langle r_E^2 \rangle_b$ with the estimates of Wang *et al.* [31]. Our results are surprisingly close to those of Ref. [31], with a notable exception for Σ^+. In this case our estimate for $\langle r_E^2 \rangle_\pi$ is 0.2 fm^2, to be compared with that of Ref. [31], -0.061 ± 0.045 fm^2, with opposite sign. In general, we conclude that our estimates for the valence quark contributions are consistent with those of Ref. [31].

In Table VII we present also the results for the bare and pion cloud contributions for the magnetic squared radii. Although the physical radii can differ appreciably from the lattice extracted radii without chiral extrapolations (see figures from 3–10), lattice results can give us an idea on the magnitude of the valence quark contributions. For this, we compare our results with those of the lattice in Ref. [65] for the lowest pion mass, $m_\pi = 306$ MeV, and Ref. [52] for $m_\pi = 354$ MeV. It is still interesting to notice that $\langle r_M^2 \rangle_b$ approach the lattice extracted values when the number of the valence strange quarks increases. The result for Σ is closer to that of the lattice than that of the nucleon, and the results for Ξ is nearly equal to that of the lattice, when the standard deviation is taken into account. This is not unexpected, since lattice QCD calculations use nearly the

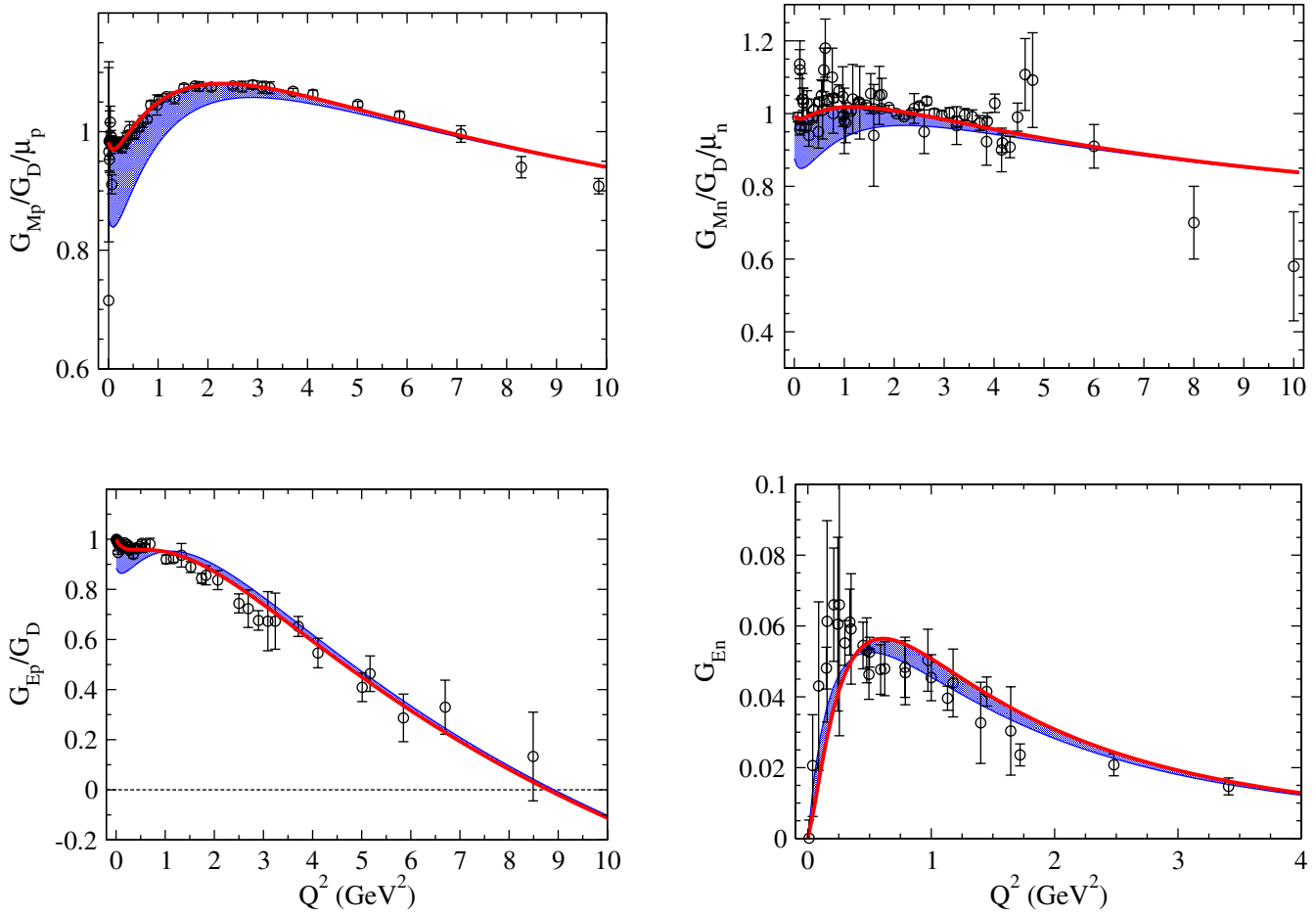

FIG. 11 (color online). Nucleon electromagnetic form factors including the sum of the bare and the pion cloud (bands). Data are from Refs. [53–64]. See text for details.

physical strange quark mass value. These facts also give us some confidence on our model to estimate the valence quark contributions both in the physical and lattice regimes.

We now comment on the neutron electric charge squared radius. Our result, -0.029 fm^2, differs appreciably from the experimental value -0.12 fm^2. This deviation is a consequence of our global fit, and the

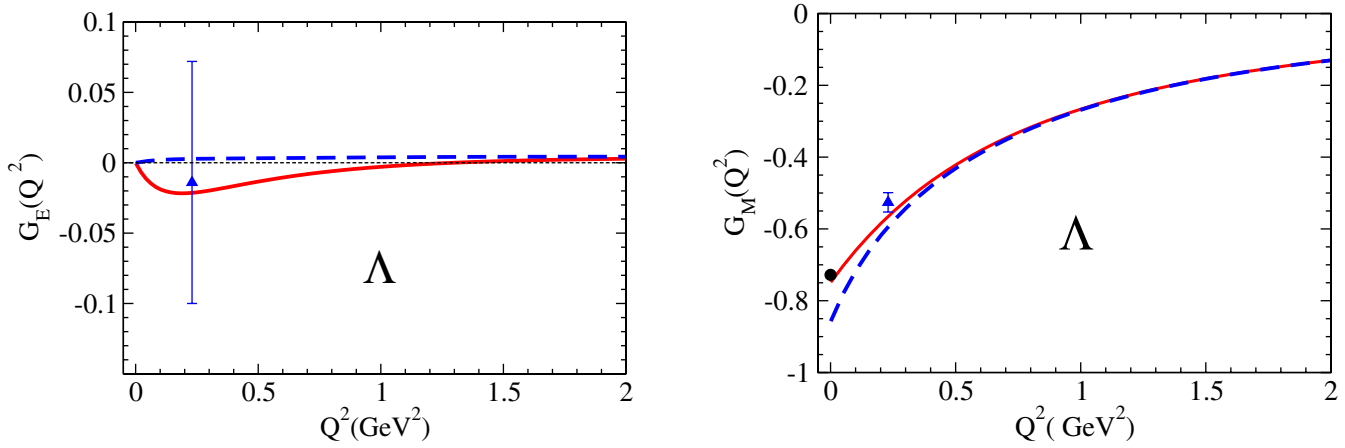

FIG. 12 (color online). Λ electromagnetic form factors for the total result (solid line) and the bare result (dashed line). The data point for $Q^2 = 0$ is the result of the magnetic moment [51]. The lattice data point (filled triangle) for $Q^2 = 0.23$ GeV^2 is from Ref. [65] ($m_\pi = 306$ MeV).

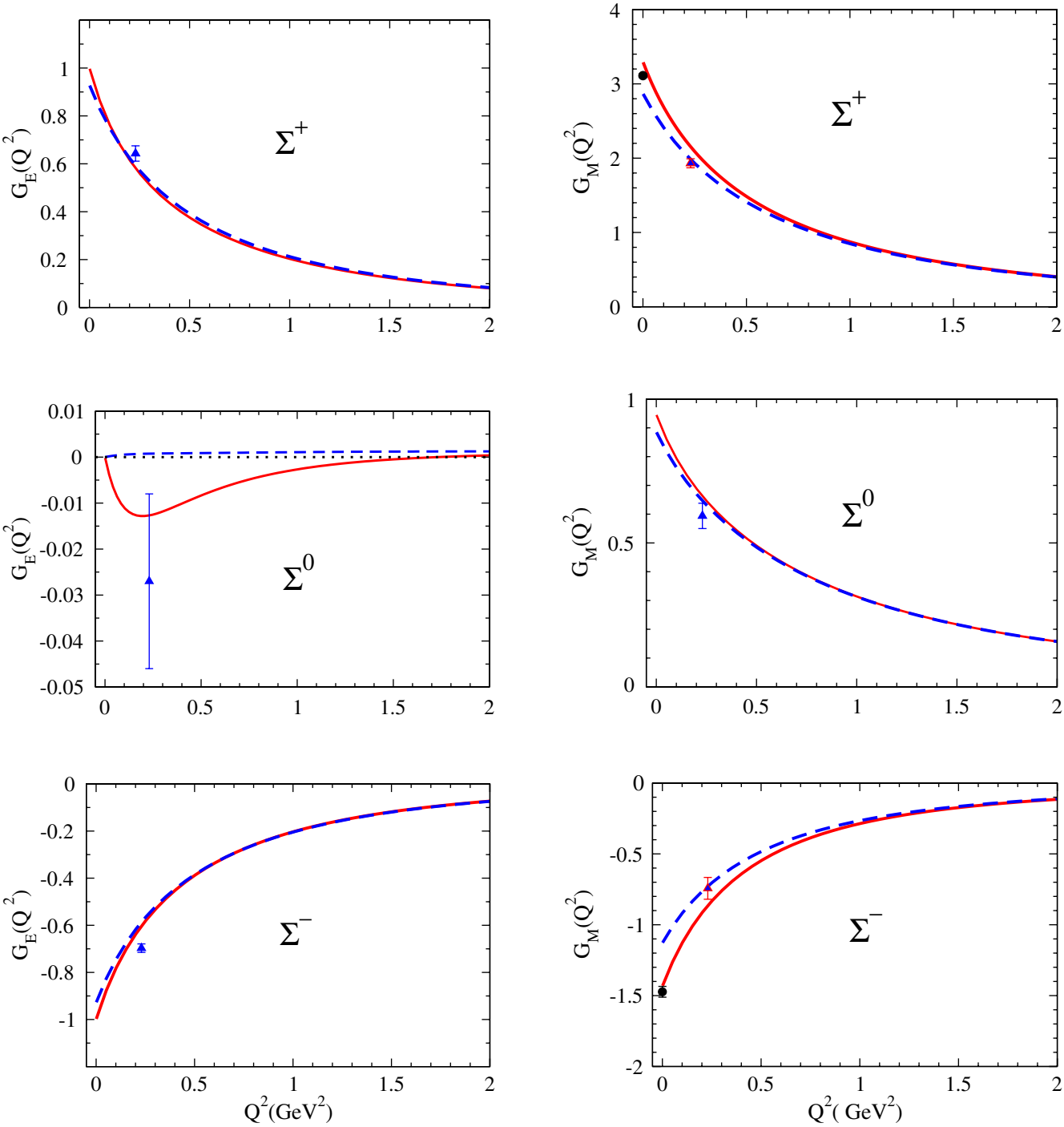

FIG. 13 (color online). Σ electromagnetic form factors for the total (solid line) and the bare result (dashed line). The data point for $Q^2 = 0$ is the result of the magnetic moment [51]. The lattice data point (filled triangle) for $Q^2 = 0.23$ GeV^2 is from Ref. [65] ($m_\pi =$ 306 MeV).

absence of high accuracy data until recently for G_{En} in the low Q^2 region [80]. The result of our fit is presented in Fig. 11, and magnified in Fig. 15 for the region $Q^2 <$ 1.5 GeV^2. As already explained, our fit includes the neutron physical data, but also includes the octet baryon lattice data. In particular, the fit also includes the lattice data for the neutron form factors G_{En} and G_{Mn}. However, since we have reduced the impact of the lattice data for the neutral particles to compensate the inaccuracy of the data, the lattice constraints to the valence quark contributions are not very strong. As a consequence, the strongest constraint for the neutron electric form factor comes from the very accurate, high Q^2 physical neutron data.

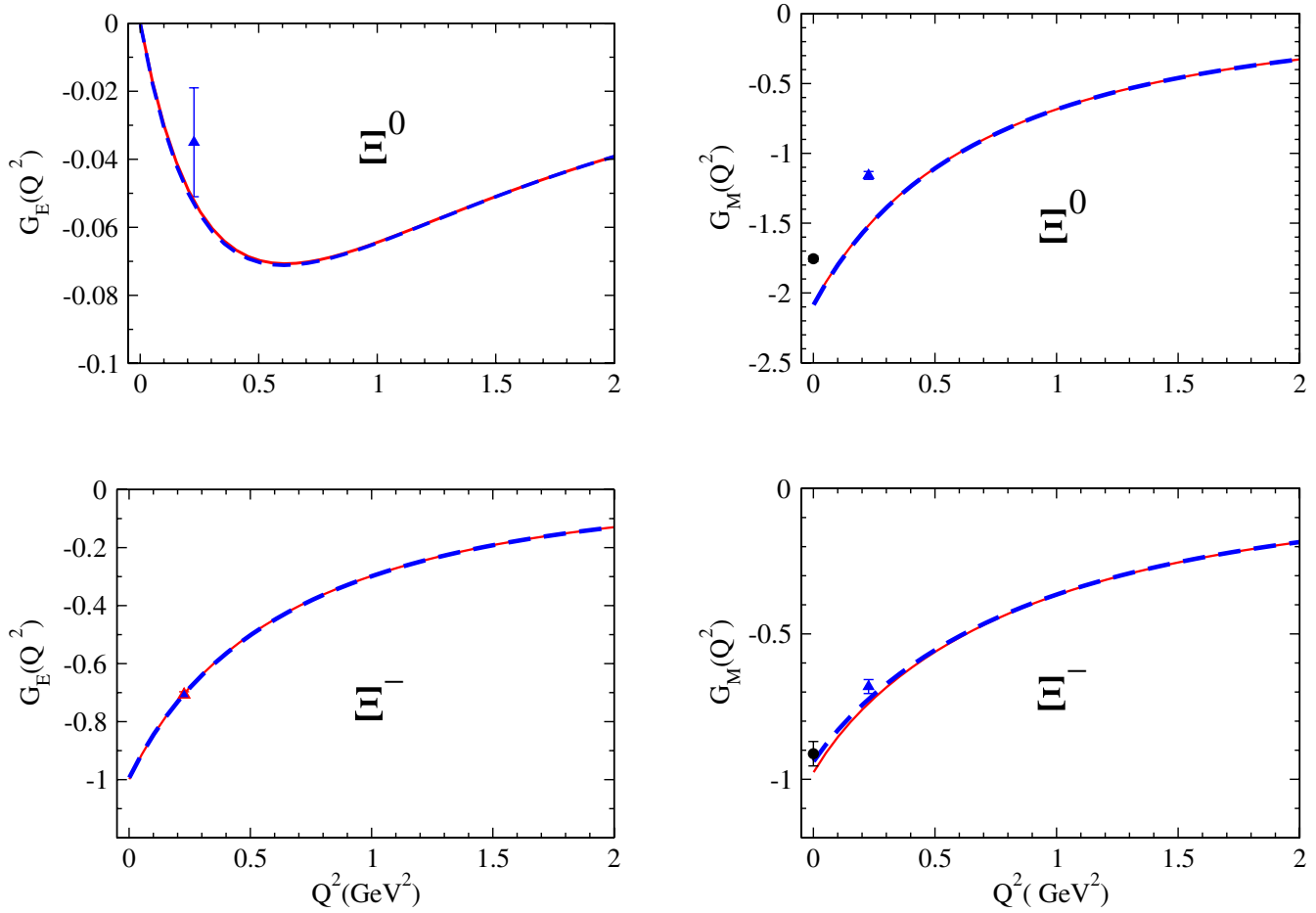

FIG. 14 (color online). Ξ electromagnetic form factors for the total result (solid line) and the bare result (dashed line). The data point for $Q^2 = 0$ is the result of the magnetic moment [51]. The lattice data point (filled triangle) for $Q^2 = 0.23$ GeV^2 is from Ref. [65] ($m_\pi = 306$ MeV).

As one can observe in Fig. 15, our model result deviates from the data in the region $Q^2 < 0.5$ GeV^2. In the figure the result associated with the valence quark contributions is closer to the data than the full result (dressed). We then conclude that the deviation of our result from the physical data is a consequence of our estimate for the pion cloud contributions, which are poorly constrained by the low Q^2 neutron physical data. In short, the poor description of G_{En} is a consequence of our ambition to describe simultaneously the lattice and physical data. It would be improved if we concentrated only on the physical data in the low Q^2 region, as done in the other studies [28]. The new generation of experiments for G_{En} with high accuracy [80] will be important to clarify the impact of the different effects in the neutron data, and can constrain quark models such as the one used in the present work. Nevertheless, our analysis shows the importance and sensitiveness of the pion cloud effects on the neutron and the neutral baryons in general. The importance of the pion cloud effects is also manifested in the results of the electric form factors of Σ^0, Λ, and Ξ^0.

TABLE VI. Electric charge squared radii of the octet baryons. All values are in fm^2. The subindexes indicate, respectively, bare (b) and pion cloud (π) contributions, as defined in the text. The experimental value presented for the proton is an average of Refs. [66–68]. An estimate of the proton electric charge squared radius using muonic hydrogen [69], gives 8% less than the result presented in the table.

	$\langle r_E^2\rangle_b$	$\langle r_E^2\rangle_\pi$	$\langle r_E^2\rangle$	Ref. [31]	Exp.
p	0.704	0.066	0.770	0.685(66)	0.769(8) [66]
n	−0.098	0.070	−0.029	−0.158(33)	−0.1161(22) [51]
Λ	−0.0081	0.091	0.082	0.010(9)	
Σ^+	0.503	0.214	0.717	0.749(72)	
Σ^0	−0.0020	0.049	0.048		
Σ^-	0.519	0.113	0.632	0.657(58)	0.61(15) [70]
Ξ^0	0.090	−0.0036	0.087	0.082(29)	
Ξ^-	0.404	0.019	0.423	0.502(47)	

VII. CONCLUSIONS

In the present work we have applied a covariant spectator quark model to study the valence quark

TABLE VII. Magnetic dipole squared radii of the octet baryons. All values are in fm^2. The experimental results are $\langle r_M^2\rangle = 0.733 \pm 0.096$ fm^2 for the proton, and $\langle r_M^2\rangle = 0.767 \pm 0.123$ fm^2 for the neutron [71]. More recent results for the proton are $\langle r_M^2\rangle = 0.604 \pm 0.026$ fm^2 [68], and $\langle r_M^2\rangle = 0.752 \pm 0.035$ fm^2 [66]. While the lattice results from Ref. [65] correspond to the pion mass $m_\pi = 306$ MeV, those from Ref. [52] correspond to $m_\pi = 354$ MeV.

	$\langle r_M^2\rangle_b$	$\langle r_M^2\rangle_\pi$	$\langle r_M^2\rangle$	Ref. [65]	Ref. [52]
p	0.679	0.059	0.738	0.470(48)	0.40(8)
n	0.714	0.0034	0.718	0.478(50)	0.46(11)
Λ	0.544	−0.242	0.302	0.347(24)	
Σ^+	0.383	0.146	0.530	0.466(42)	0.36(8)
Σ^0	0.365	0.103	0.468	0.423(38)	
Σ^-	0.407	0.199	0.606	0.483(49)	0.37(8)
Ξ^0	0.370	−0.0010	0.368	0.384(22)	0.32(2)
Ξ^-	0.295	0.045	0.340	0.336(18)	0.29(4)

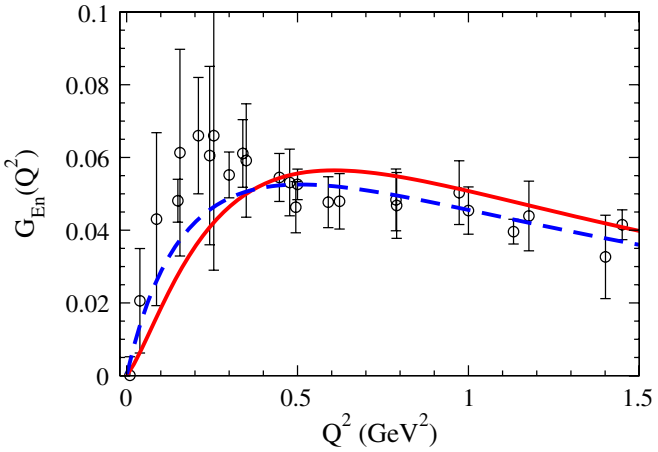

FIG. 15 (color online). Neutron electric form factor in the low Q^2 region (magnified from Fig. 11). The lines are for the total result (solid line) and the bare result (dashed line).

structure of the octet baryons. Combining the contributions of the valence quarks (covariant model) with a phenomenological, covariant parametrization for the pion cloud contributions, we have described the electromagnetic form factors of the octet baryons in the lattice and physical regimes. The octet baryon systems are described in a simplified quark model with the S-state configuration for the quark-diquark relative motion. The simplicity of the wave functions allows us to calibrate the momentum dependence of the octet baryon form factors using four independent range parameters. The model has been calibrated using lattice QCD data for the octet baryons (272 data points), the physical nucleon form factor data (202 data points), and the physical octet baryon magnetic moment data (5 data points). Overall, we have used 6 parameters for the valence quark structure, and 7 parameters for the pion cloud effects. We have derived a parametrization for the octet baryon wave functions depending on the baryon flavors. The parametrized wave functions are very useful for future studies of the electromagnetic reactions.

TABLE VIII. Valence quark contributions for the octet baryon electric charge squared radii, compared with the valence quark contributions from Ref. [31], and lattice QCD simulations [52,65]. While the lattice results from Ref. [65] correspond to the pion mass $m_\pi = 306$ MeV, those from Ref. [52] correspond to $m_\pi = 354$ MeV.

	$\langle r_E^2\rangle_b$	Ref. [31]	Ref. [65]	Ref. [52]
p	0.704	0.746(69)	0.452(53)	0.41(4)
n	−0.098	−0.097(31)	0.029(41)	
Λ	−0.0081	0.026(9)	0.025(7)	
Σ^+	0.503	0.820(75)	0.503(54)	0.44(3)
Σ^0	−0.0020		0.046(15)	
Σ^-	0.519	0.586(56)	0.410(37)	0.357(16)
Ξ^0	0.090	0.113(27)	0.062(22)	
Ξ^-	0.404	0.471(46)	0.389(23)	0.326(6)

Our results suggest a dominance of the valence quark effects, but the inclusion of the pion cloud effects improves the global description of the octet baryon electromagnetic form factor data. The pion cloud effects are of the order of 15% for the nucleon in the low Q^2 region, but decrease in the higher Q^2 region. Surprisingly, the pion cloud effects are still important for the nucleon electric form factors in the region of 5–10 GeV^2 with the contributions of 5–8%. This feature is a consequence of the value of Λ_2 ($\Lambda_2^2 = 1.54$ GeV^2) for the pion cloud parametrization, which gives a slow falloff for the Pauli form factor F_2.

We have a good description of the nucleon data (χ^2 per data point $\simeq 1.9$), but for the description of the neutron it is slightly worse (χ^2 per data point of 1.9 and 2.3 for the electric and magnetic form factors, respectively). This is a consequence of the high accuracy of the recent G_{Mn} data [64], and also our ambition to describe simultaneously the lattice and physical data. The large number of the lattice data points reduces the impact of the nucleon physical data. Also the inaccuracy of the neutron lattice data (especially differs from the neutron charge zero at $Q^2 = 0$) makes it difficult to constrain those parameters of the model directly related to the nucleon system. To improve the description of the nucleon system, it will be useful to perform a more systematic and detailed study for the nucleon form factors. This can be done using a more complete lattice QCD database including the results from Refs. [81–86], and also the results of the new generation of nucleon form factor data in the low Q^2 region [80,87,88], which determine G_E and G_M simultaneously instead of the ratio[6]

[6]That will require the combination of the polarization transfer measurements and cross section measurements (Rosenbluth method).

G_E/G_M. In this work we have restricted to use the lattice data from Ref. [52], since one of our goals is the overall description of the octet baryon electromagnetic structure, and we prefer to avoid possible inconsistencies arising from different lattice QCD simulations.

Our results for the neutron form factors require some discussions. Our global fit has turned up to give a poor description for the neutron electric form factor for $Q^2 < 0.5$ GeV^2 (electric charge squared radius of -0.029 fm^2). Although G_{En} is poorly constrained by the lattice data, it is complemented by the physical data. Our result for the neutron electric squared radius differs appreciably from the experimental value, although our estimate of the bare valence quark core is closer to the experimental value, and also to that of the valence quark contribution from Ref. [31]. We interpret this as a consequence of the impact of the high Q^2 region data (very precise in general), which reduce the impact of the low Q^2 region data (less accurate) in the global fit. As already discussed, a more precise calibration of the model for the neutron will require a more detailed analysis of the nucleon system, and this will be possible when more precise data as in Ref. [80] become available. More accurate lattice QCD data for the neutron can also be very useful. Nevertheless, our results show that the pion cloud effects are indeed important and influential for the neutron data.

Overall, we have a very good global description of both the lattice QCD and physical data for the charged particles p, $\Sigma^{\pm}$, and Ξ^-. For the analysis of neutral particles, one must be careful, because they have been less constrained by the lattice data (n and Ξ^0), or not at all constrained (Λ and Σ^0). But we can conclude that the pion cloud effects are very important for the electromagnetic form factors G_{EB} of neutral particles.

Concerning the size of the octet baryons, we conclude that, as expected, the systems with two strange quarks are more compact than those of the one strange quark, and the latter is more compact than the nucleon system with no strange quark. The estimates of the octet baryon sizes (electric charge squared and magnetic dipole squared radii) due to the valence quarks (bare core) are consistent with this conclusion, and are also in agreement with the independent estimates [31]. The inclusion of the pion cloud effects in the electric charge squared radii, in general, makes the final results approach to the experimental results, and also to the values estimated based on the lattice results extrapolated using chiral perturbation theory [31].

The agreement between our estimates with the octet baryon electromagnetic form factor data, and also those of the radii, gives us some confidence about the applicability of our model to estimate the valence quark effects both in the physical and lattice regimes. An application of the present model for the octet to decuplet electromagnetic transitions is in progress by generalizing the study made for the $\gamma N \to \Delta$ transition [18–20]. For this purpose, we can use the octet baryon wave functions obtained in this work, and those of the decuplet obtained in Ref. [3] within the same formalism [89].

ACKNOWLEDGMENTS

The authors would like to thank Jerry Gilfoyle for providing the data from Ref. [64]. This work was supported in part by the European Union (HadronPhysics2 project "Study of Strongly Interacting Matter"). This work was also supported by the University of Adelaide and the Australian Research Council through Grant No. FL0992247 (AWT). G. R. was supported by the Fundação para a Ciência e a Tecnologia under Grant No. SFRH/BPD/26886/2006.

APPENDIX: BRIEF REVIEW OF NUCLEON ELECTROMAGNETIC FORM FACTORS

Here we briefly review the results of Ref. [1] for the nucleon electromagnetic form factors. We consider the wave function from Eq. (4), corresponding to the nucleon case (see Ref. [1] for details). Below, M_N represents the nucleon mass.

In the following we use

$$\Delta^{\alpha\beta} = \sum_{\lambda} \varepsilon^{\alpha}_{P_+}(\lambda)\varepsilon^{\beta *}_{P_-}(\lambda), \tag{A1}$$

where $\varepsilon_{P_\pm}$ is the diquark polarization vectors of the final (P_+) and initial (P_-) states in the fixed-axis representation [35]. The direct calculation gives [1,18,35]

$$\Delta^{\alpha\beta} = -\left(g^{\alpha\beta} - \frac{P_-^{\alpha}P_+^{\beta}}{P_+\cdot P_-}\right) + a\left(P_-^{\alpha} - \frac{P_+\cdot P_-}{M_+^2}P_+^{\alpha}\right)\left(P_+^{\beta} - \frac{P_+\cdot P_-}{M_-^2}P_-^{\beta}\right), \tag{A2}$$

with

$$a = -\frac{M_+M_-}{P_+\cdot P_-(M_+M_- + P_+\cdot P_-)}, \tag{A3}$$

where M_- and M_+ are the masses of the initial and final states. In the present case $M_+ = M_- = M_N$.

Equation (11) leads to the transition current [1],

$$J_N^{\mu} = \frac{3}{2}B(Q^2)\times\bar{u}(P_+)\left\{\left[j_1\gamma^{\mu} + j_2\frac{i\sigma^{\mu\sigma}q_{\sigma}}{2M_N}\right] - \frac{1}{3}\gamma_{\alpha}\gamma_5\left[j_3\gamma^{\mu} + j_4\frac{i\sigma^{\mu\sigma}q_{\sigma}}{2M_N}\right]\gamma_5\gamma_{\beta}\Delta^{\alpha\beta}\right\}u(P_-), \tag{A4}$$

where $\Delta^{\alpha\beta}$ is given by Eq. (A2), and

$$B(Q^2) = \int_k \psi_N(P_+,k)\psi_N(P_-,k). \tag{A5}$$

The coefficients, j_1 and j_2, can be written in the SU(2) sector,

$$j_i = \frac{1}{6} f_{1+}(Q^2) + \frac{1}{2} f_{1-}(Q^2)\tau_3, \tag{A6}$$

and

$$j_{(i+2)} = \frac{1}{3}\tau_j j_i \tau_j = \frac{1}{6} f_{1+} - \frac{1}{6} f_{1-}\tau_3. \tag{A7}$$

Note that the expressions (A6) and (A7), when applied to the nucleon isospin state

$$\chi_+ = \begin{pmatrix} 1 \\ 0 \end{pmatrix}$$

and

$$\chi_- = \begin{pmatrix} 0 \\ 1 \end{pmatrix},$$

are equivalent to Eqs. (17) and (18).

With some spin algebra we obtain

$$F_1(Q^2) = \frac{3}{2} B(Q^2)\left\{ j_1 + \frac{1}{3}\frac{1}{4M_N^2 + Q^2}[(12M_N^2 - Q^2) j_3 - 4Q^2 j_4]\right\}, \tag{A8}$$

$$F_2(Q^2) = \frac{3}{2} B(Q^2)\left\{ j_2 - \frac{1}{3}\frac{1}{4M_N^2 + Q^2}[16M_N^2 j_3 + (4M_N^2 - 3Q^2) j_4]\right\}. \tag{A9}$$

To extend these results to the octet baryon B, we use M_B for its mass, and make the replacements

$$j_1 \to j_1^A, \tag{A10}$$

$$j_2 \to \frac{M_B}{M_N} j_2^A, \tag{A11}$$

$$j_3 \to j_1^S, \tag{A12}$$

$$j_4 \to \frac{M_B}{M_N} j_2^S. \tag{A13}$$

The expressions associated with j_1 and j_3 are determined directly from the respective definitions. For j_2 and j_4, we need to take into account that the quark current Eq. (14) is written in terms of the nucleon mass, which leads to

$$\frac{i\sigma^{\mu\nu} q_\mu}{2M_N} = \frac{M_B}{M_N}\frac{i\sigma^{\mu\nu} q_\mu}{2M_B}. \tag{A14}$$

That is why the coefficients $j_2^{A,S}$ are modified by the factor $\frac{M_B}{M_N}$. Finally, in Eq. (A5) we replace ψ_N by ψ_B.

[1] F. Gross, G. Ramalho, and M. T. Peña, Phys. Rev. C **77**, 015202 (2008).
[2] F. Gross, G. Ramalho, and K. Tsushima, Phys. Lett. B **690**, 183 (2010).
[3] G. Ramalho, K. Tsushima, and F. Gross, Phys. Rev. D **80**, 033004 (2009).
[4] K. Kubodera, Y. Kohyama, K. Oikawa, and C. W. Kim, Nucl. Phys. **A439**, 695 (1985); Y. Kohyama, K. Oikawa, C. W. Kim, and K. Kubodera, Prog. Theor. Phys. **73**, 1278 (1985).
[5] J. F. Donoghue, B. R. Holstein, and S. W. Klimt, Phys. Rev. D **35**, 934 (1987).
[6] Y. Kohyama, K. Oikawa, K. Tsushima, and K. Kubodera, Phys. Lett. B **186**, 255 (1987); K. Tsushima, T. Yamaguchi, M. Takizawa, Y. Kohyama, and K. Kubodera, Phys. Lett. B **205**, 128 (1988); K. Tsushima, T. Yamaguchi, Y. Kohyama, and K. Kubodera, Nucl. Phys. **A489**, 557 (1988); T. Yamaguchi, K. Tsushima, Y. Kohyama, and K. Kubodera, Nucl. Phys. **A500**, 429 (1989).
[7] R. Jakob, P. Kroll, M. Schurmann, and W. Schweiger, Z. Phys. A **347**, 109 (1993).
[8] H. C. Kim, A. Blotz, M. V. Polyakov, and K. Goeke, Phys. Rev. D **53**, 4013 (1996).
[9] R. A. Williams and C. Puckett-Truman, Phys. Rev. C **53**, 1580 (1996).
[10] B. Kubis, T. R. Hemmert, and U. G. Meissner, Phys. Lett. B **456**, 240 (1999).
[11] B. Kubis and U. G. Meissner, Eur. Phys. J. C, **18**, 747 (2001).
[12] S. Cheedket, V. E. Lyubovitskij, T. Gutsche, A. Faessler, K. Pumsa-ard, and Y. Yan, Eur. Phys. J. A **20**, 317 (2004).
[13] A. Silva, Ph.D. thesis, University of Buchum, 2004.
[14] L. Wang and F. X. Lee, Phys. Rev. D **78**, 013003 (2008).
[15] Y. L. Liu and M. Q. Huang, Phys. Rev. D **80**, 055015 (2009).
[16] Y. L. Liu and M. Q. Huang, Phys. Rev. D **79**, 114031 (2009).
[17] C. F. Perdrisat, V. Punjabi, and M. Vanderhaeghen, Prog. Part. Nucl. Phys. **59**, 694 (2007).
[18] G. Ramalho, M. T. Peña, and F. Gross, Eur. Phys. J. A **36**, 329 (2008).
[19] G. Ramalho, M. T. Peña, and F. Gross, Phys. Rev. D **78**, 114017 (2008).
[20] G. Ramalho and M. T. Peña, Phys. Rev. D **80**, 013008 (2009).

[21] H. W. Hammer, D. Drechsel, and U. G. Meissner, Phys. Lett. B **586**, 291 (2004); U. G. Meissner, AIP Conf. Proc. **904**, 142 (2007).
[22] N. Kaiser, Phys. Rev. C **68**, 025202 (2003).
[23] D. B. Leinweber, D. H. Lu, and A. W. Thomas, Phys. Rev. D **60**, 034014 (1999).
[24] S. Theberge and A. W. Thomas, Nucl. Phys. **A393**, 252 (1983).
[25] A. W. Thomas, Adv. Nucl. Phys. **13**, 1 (1984).
[26] D. H. Lu, A. W. Thomas, and A. G. Williams, Phys. Rev. C **57**, 2628 (1998); D. H. Lu, S. N. Yang, and A. W. Thomas, Nucl. Phys. **A684**, 296 (2001).
[27] G. A. Miller, Phys. Rev. C **66**, 032201 (2002).
[28] J. Friedrich and T. Walcher, Eur. Phys. J. A **17**, 607 (2003).
[29] A. Faessler, T. Gutsche, V. E. Lyubovitskij, and K. Pumsaard, Phys. Rev. D **73**, 114021 (2006).
[30] P. Wang, D. B. Leinweber, A. W. Thomas, and R. D. Young, Phys. Rev. D **75**, 073012 (2007).
[31] P. Wang, D. B. Leinweber, A. W. Thomas, and R. D. Young, Phys. Rev. D **79**, 094001 (2009).
[32] I. C. Cloet, G. Eichmann, B. El-Bennich, T. Klahn, and C. D. Roberts, Few Body Syst. **46**, 1 (2009).
[33] G. Ramalho and M. T. Peña, J. Phys. G **36**, 115011 (2009).
[34] F. Gross, Phys. Rev. **186**, 1448 (1969); F. Gross, J. W. Van Orden, and K. Holinde, Phys. Rev. C **45**, 2094 (1992).
[35] F. Gross, G. Ramalho, and M. T. Peña, Phys. Rev. C **77**, 035203 (2008).
[36] G. Ramalho and M. T. Peña, J. Phys. G **36**, 085004 (2009).
[37] G. Ramalho, M. T. Peña, and F. Gross, Phys. Lett. B **678**, 355 (2009).
[38] G. Ramalho, M. T. Peña, and F. Gross, Phys. Rev. D **81**, 113011 (2010).
[39] G. Ramalho and M. T. Peña, Phys. Rev. D **83**, 054011 (2011).
[40] G. Ramalho and K. Tsushima, Phys. Rev. D **81**, 074020 (2010).
[41] G. Ramalho, F. Gross, M. T. Peña, and K. Tsushima, in *Proceedings of the 4th Workshop on Exclusive Reactions at High Momentum Transfer, 2011*, edited by Anatoly Radyushkin (World Scientific, Singapore, 2011), p. 287.
[42] G. Ramalho and K. Tsushima, Phys. Rev. D **82**, 073007 (2010).
[43] G. Ramalho and M. T. Peña, Phys. Rev. D **84**, 033007 (2011).
[44] G. Ramalho and K. Tsushima, Phys. Rev. D **84**, 051301(R) (2011).
[45] W. Detmold, D. B. Leinweber, W. Melnitchouk, A. W. Thomas, and S. V. Wright, Pramana **57**, 251 (2001); J. D. Ashley, D. B. Leinweber, A. W. Thomas, and R. D. Young, Eur. Phys. J. A **19**, 9 (2004).
[46] G. Ramalho and K. Tsushima (work in progress).
[47] M. Gell-Mann, Phys. Rev. **125**, 1067 (1962).
[48] P. Carruthers, *Introduction to Unitary Symmetry* (John Wiley and Sons, New York, 1966), p. 118.
[49] D. B. Leinweber, A. W. Thomas, K. Tsushima, and S. V. Wright, Phys. Rev. D **64**, 094502 (2001).
[50] S. J. Brodsky and G. R. Farrar, Phys. Rev. D **11**, 1309 (1975).
[51] C. Amsler *et al.* (Particle Data Group), Phys. Lett. B **667**, 1 (2008).
[52] H. W. Lin and K. Orginos, Phys. Rev. D **79**, 074507 (2009).
[53] M. K. Jones *et al.* (Jefferson Lab Hall A Collaboration), Phys. Rev. Lett. **84**, 1398 (2000); O. Gayou *et al.* (Jefferson Lab Hall A Collaboration), Phys. Rev. Lett. **88**, 092301 (2002).
[54] A. J. R. Puckett *et al.*, Phys. Rev. Lett. **104**, 242301 (2010).
[55] J. Arrington, W. Melnitchouk, and J. A. Tjon, Phys. Rev. C **76**, 035205 (2007).
[56] M. Ostrick *et al.*, Phys. Rev. Lett. **83**, 276 (1999); C. Herberg *et al.*, Eur. Phys. J. A **5**, 131 (1999); D. I. Glazier *et al.*, Eur. Phys. J. A **24**, 101 (2005).
[57] I. Passchier *et al.*, Phys. Rev. Lett. **82**, 4988 (1999).
[58] T. Eden *et al.*, Phys. Rev. C **50**, R1749 (1994).
[59] H. Zhu *et al.* (E93-026 Collaboration), Phys. Rev. Lett. **87**, 081801 (2001); R. Madey *et al.* (E93-038 Collaboration), Phys. Rev. Lett. **91**, 122002 (2003); G. Warren *et al.* (E93-026 Collaboration), Phys. Rev. Lett. **92**, 042301 (2004).
[60] S. Riordan *et al.*, Phys. Rev. Lett. **105**, 262302 (2010).
[61] R. Schiavilla and I. Sick, Phys. Rev. C **64**, 041002 (2001).
[62] P. E. Bosted, Phys. Rev. C **51**, 409 (1995).
[63] G. Kubon *et al.*, Phys. Lett. B **524**, 26 (2002); H. Anklin *et al.*, Phys. Lett. B **428**, 248 (1998); **336**, 313 (1994).
[64] J. Lachniet *et al.* (CLAS Collaboration), Phys. Rev. Lett. **102**, 192001 (2009).
[65] S. Boinepalli, D. B. Leinweber, A. G. Williams, J. M. Zanotti, and J. B. Zhang, Phys. Rev. D **74**, 093005 (2006).
[66] X. Zhan, arXiv:1102.0318.
[67] P. J. Mohr, B. N. Taylor, and D. B. Newell, Rev. Mod. Phys. **80**, 633 (2008).
[68] J. C. Bernauer *et al.* (A1 Collaboration), Phys. Rev. Lett. **105**, 242001 (2010).
[69] R. Pohl *et al.*, Nature (London) **466**, 213 (2010).
[70] I. M. Gough Eschrich *et al.* (SELEX Collaboration), Phys. Lett. B **522**, 233 (2001).
[71] G. G. Simon, C. Schmitt, F. Borkowski, and V. H. Walther, Nucl. Phys. **A333**, 381 (1980).
[72] J. Kunz and P. J. Mulders, Phys. Rev. D **41**, 1578 (1990).
[73] C. Gobbi, S. Boffi, and D. O. Riska, Nucl. Phys. **A547**, 633 (1992).
[74] A. R. Panda, K. C. Roy, and R. K. Sahoo, Phys. Rev. D **49**, 4659 (1994).
[75] G. Wagner, A. J. Buchmann, and A. Faessler, Phys. Lett. B **359**, 288 (1995).
[76] S. J. Puglia, M. J. Ramsey-Musolf, and S. L. Zhu, Phys. Rev. D **63**, 034014 (2001).
[77] A. J. Buchmann and R. F. Lebed, Phys. Rev. D **67**, 016002 (2003).
[78] A. J. Buchmann, in *Proceedings of the IX International Conference on Hypernuclear and Strange Particle Physics, Hyp 2006, Mainz, Germany, 2006*, edited by J. Pochodzalla and Th. Walcher (Springer-Verlag, Berlin, 2007).
[79] H. Dahiya and N. Sharma, AIP Conf. Proc. **1322**, 445 (2010).
[80] E. Geis *et al.* (BLAST Collaboration), Phys. Rev. Lett. **101**, 042501 (2008).
[81] M. Gockeler, T. R. Hemmert, R. Horsley, D. Pleiter, P. E. L. Rakow, A. Schafer, and G. Schierholz (QCDSF Collaboration), Phys. Rev. D **71**, 034508 (2005).

[82] C. Alexandrou, G. Koutsou, J. W. Negele, and A. Tsapalis, Phys. Rev. D **74**, 034508 (2006).
[83] C. Alexandrou, G. Koutsou, H. Neff, J. W. Negele, W. Schroers, and A. Tsapalis, Phys. Rev. D **77**, 085012 (2008).
[84] S. N. Syritsyn *et al.*, Phys. Rev. D **81**, 034507 (2010).
[85] H. W. Lin, S. D. Cohen, R. G. Edwards, K. Orginos, and D. G. Richards, arXiv:1005.0799.
[86] S. Collins *et al.*, arXiv:1106.3580.
[87] G. Ron *et al.*, arXiv:1103.5784.
[88] S. Gilad (Jefferson Lab Hall A Collaboration), Few Body Syst. **50**, 451 (2011).
[89] G. Ramalho and K. Tsushima (work in progress).